11-7-2007

Design and Modeling of a Bistable Spherical Compliant Micromechanism

Joseph Georges Choueifati
University of South Florida

Design and Modeling of a Bistable Spherical Compliant Micromechanism

by

Joseph Georges Choueifati

A thesis submitted in partial fulfillment
of the requirements for the degree of
Master of Science in Mechanical Engineering
Department of Mechanical Engineering
College of Engineering
University of South Florida

Major Professor: Craig Lusk, Ph.D.
Daniel Hess, Ph.D.
Jose Porteiro, Ph.D.

Date of Approval:
November 7, 2007

Keywords: (Bistable, spherical, compliant)

Dedication

To my Father, Georges, my Mother, Amal, my Brother, Jules,
and my Sister, Joelle.

Acknowledgments

I would like to express my gratitude to my major professor Dr. Craig Lusk for his continuous support during this journey. He has been more than a mentor; he has been a good friend. His patience and expertise were key factors in the completion of this thesis. It was a great privilege working under his direction.

I would like to thank my graduate committee for their time spent on my behalf: Dr. Hess, and Dr. Porteiro. Their guidance was invaluable. Fellow graduate students and friends Alejandro Leon, Carlos F. Acosta, Vivek Ramadoss, Christopher Cheatham, Michael Nellis and Antoine Awwad for the moral support provided. Special recognition should be given to my family for supporting and motivating me through it all. Without them, I would not be where I am today.

Table of Contents

List of Tables

List of Figures

Design and Modeling of a Bistable Spherical Compliant Micromechanism

Joseph Georges Choueifati

ABSTRACT

Compliant bistable mechanisms are mechanisms that have two stable equilibrium positions within their range of motion. Their bistability is mainly due to a combination of the elasticity of their members and their force transmission properties. This thesis introduces a new type of bistable micromechanisms, the Bistable, Spherical, Compliant, four-bar Micromechanism (BSCM). Theory to predict bistable positions and configurations is also developed. Bistabilty was demonstrated through testing done on micro-prototypes. Compared to the mathematical model of the BSCM, Finite element models of the BSCM indicated important qualitative differences in the mechanism's stability behavior and its input-angle-input torque relation. The BSCM has many valuable features, such as: two stable positions that require power only when moving from one stable position to the other, precise and repeatable out-of-plane motion with resistance to small perturbations. The BSCM may be useful in several applications such as active Braille systems and Digital Light Processing (DLP) chips.

Chapter 1

1.1 Objective

The objective of this research was to develop a bistable Micro-electro-mechanical system with precise and repeatable out of plane motion. Combining spherical mechanism theory and compliant mechanism theory, large out of plane motion can be achieved. To insure its precision and repeatability, the mechanism was designed to have two stable equilibrium positions.

The theory developed was demonstrated through testing performed on macro and micro-scaled devices that were designed, fabricated and analyzed as part of this research. Finite-element analysis (FEA) was used to predict the motion and bistable behavior of the mechanism. Possible applications for such a mechanism were also considered.

1.2 Motivation

The most common technique used in building MEMS is surface micromachining [1, 2] because of its simplicity and low cost. A challenge in using surface micromachining is that the process produces essentially two dimensional products. The ratio of the length and width with respect to the thickness of the

elements created is high, thus most MEMS have a planar working space, where the motion of their links traces a single plane, [3]. In some applications such as active Braille [4], micro-optical systems [5], it may be useful for MEMS to achieve accurate three-dimensional motion.

1.3 Contribution

The research in this thesis provides a new design in the MEMS field. A bistable spherical compliant four-bar micromechanism. The theory for modeling the mechanism is presented. Microprototypes were designed and fabricated using the Multi Users MEMS Process (MUMPs) to insure feasibility and theory verification. For further understanding of the mechanism's behavior several models were developed.

1.4 Research Approach

The next chapter, Chapter 2, provides a background on MEMS and MEMS applications and their impact on today's technology. In Chapter 3 mathematical background useful in describing the mechanisms is presented. Chapter 4 presents the mathematical model of a bistable spherical compliant four-bar mechanism (BSCM). In Chapter 5 a MEMS prototype of the BSCM is presented and test results are discussed with an FEA analysis of several configurations of the MEMS prototype. Chapter 6 provides conclusions and future recommendations.

Chapter 2

Introduction

2.1 MEMS History

For the past two decades, integrated circuit technology has enabled researchers and scientists to create micro-scaled machines that can interact with their environment mechanically and electronically on the micro scale. These systems are called Microelectromechanical Systems (MEMS) and are being used in several industrial areas and are being integrated in devices that are used in our everyday life. One of the most successful commercialization stories of MEMS is that of the airbag accelerometer. In a four year period, form 1995 to 1999, the airbag accelerometer market share skyrocketed from 20% to 80%, and saved automobile manufacturers 50$ per car [6]. Another prominent use of MEMS is the Texas Instruments Digital Light Processor (DLP) chip, which the core component of the high definition Samsung DLP projection TVs currently being sold on the market. The DLP chip is probably the world's most sophisticated light switch. It contains a rectangular array of up to 2 million hinge-mounted digital micro-mirror devices (DMD); each of these micro-mirrors measures less than one-fifth the width of a human hair. These DMD are manipulated by MEMS with accurate but limited out of plane motion [7]. Moreover, because of their small dimensions, power requirements to activate MEMS are small and usually fall on

the mW scale. Predicted future applications of MEMS range from the aerospace industry, where MEMS will be integrated in navigation systems, to the medical industry where micro-manipulator may operate on cells [1]. Briefly, a typical MEMS device can be defined as: (1) device consisting of micro-mechanisms and/or microelectronics, (2) a device that can be batch fabricated, and (3) a device that does not require a great deal of assembly to utilize its functionality. [8]

2.2 Background

2.2.1 Surface Micromachining

The most common technique used in building MEMS is surface micromachining because of its simplicity and low cost. In surface micromachining, the silicon wafer acts as the substrate, on which multiple layers of thin layers of polysilicon or silicon nitride are built [1, 2]. A significant challenge of using surface micromachining, is that it is a two dimensional process. The elements created can measure in length and width several hundred microns but in thickness less than 10 microns, making them relatively planar. Thus most MEMS have a planar working space [3]. For many of the applications mentioned above it may be necessary for MEMS to achieve three-dimensional motion. To achieve that goal, researchers are required to come up with creative designs.

2.2.2 Ortho-Planar Mechanisms

Ortho-planar (OP) mechanisms [9] are a type of mechanism that can achieve out-of-plane motion. Ortho-Planar mechanisms are defined as

mechanisms that are built with their links located in a single plane and motion out of that plane [9]. In his dissertation, Lusk describes numerous types of OP MEMS and spherical MEMS. See examples in Figures 2.1 and 2.2

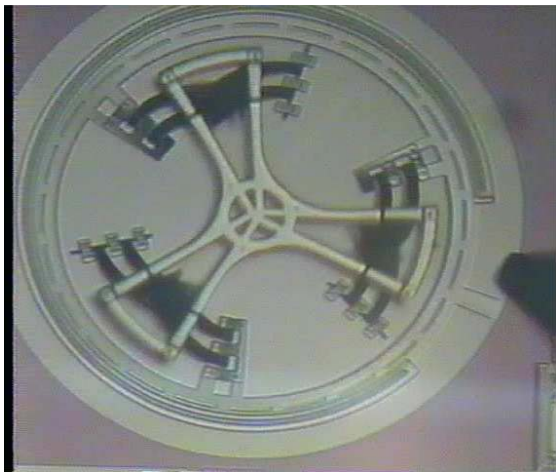

Figure 2.1: Ortho-Planar Spherical Mechanism [3]

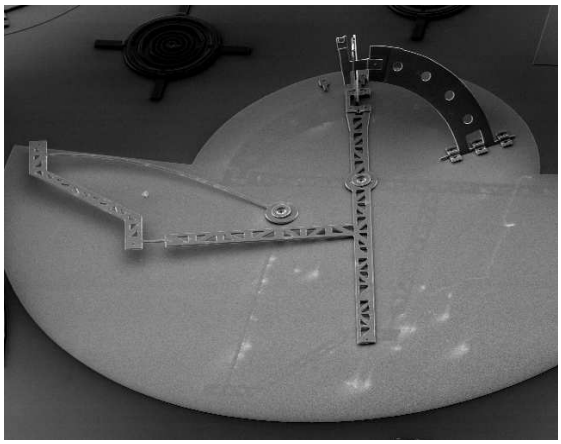

Figure 2.2: Spherical Bistable Mechanism [3]

2.2.3 Spherical Mechanisms

A spherical mechanism is a mechanism where the axes of rotation of all its revolute joints intersect at a single point. The shortest distance between this point and any of the mechanism's joints corresponds to the radius of a sphere that is the virtual workspace of that mechanism. Further information on spherical mechanisms is given in Chapters Three and Four.

One particular application where the use of spherical MEMS with accurate out-of plane motion might be important is in DLP chips. Indeed, DMDs are tilted back and forth into their ON/OFF positions by MEMS. The maximum tilt angle reached at the present is 12 degrees. According to Texas Instruments, the higher the tilt angle, the better the resolution. Another application where spherical MEMS may be important is in Micro Input Devices Systems (MIDS). MIDS can be integrated in braille-based typing system that interacts differently with each finger motion pattern. The computer will then translate different patterns into words [4].

In order to achieve these results, designs are needed that allow for rapid, large and accurate spatial positioning of arrays of micro-mirrors. According to Fukushige: *If a long stroke in the out-of-plane direction, a large output force, and high integration can be simultaneously realized, micro-optical systems such as actuation of micro-mirrors become possible"* [5]. This thesis offers a detailed analysis of a MEMS device with large displacement and precise out-of-plane motion.

2.2.4 Compliant Mechanisms

With the manufacturing techniques available at their hands and an understanding of MEMS challenges, researchers are able to develop elastically deformable micro structures [10]. Mechanisms that rely on elastic deformation of their flexural members to carry out mechanical tasks of transforming and transferring energy force and motion are called *compliant mechanisms* [10]. Furthermore, compliant mechanisms combine energy storage and motion, thus eliminating the need for separate components of joints and springs [10]. Many products currently on the market such as nail clippers, shampoo caps and mechanical pens make use of compliant segments in their designs. In addition, studies have shown that one of the main reasons behind the failure of MEMS is joints wear [11]; and that replacing these rigid multi-pieces joints with compliant single member joint will likely increase their lifespan [12,13,14]. On the other hand; the advantages offered by compliant micromechanisms don't come without challenges. Their dynamic and kinematics analysis is difficult but can be simplified using easier techniques such as the Pseudo-rigid-body model (PRBM) [14].

PRBMs model compliant mechanisms as rigid-body mechanisms. They can predict with high accuracy the nonlinear large deflections of flexible segments [15]. Chapter 3 offers a more elaborate background on PRBM. The use of the PRBM will be discussed in more depth in Chapter 3.

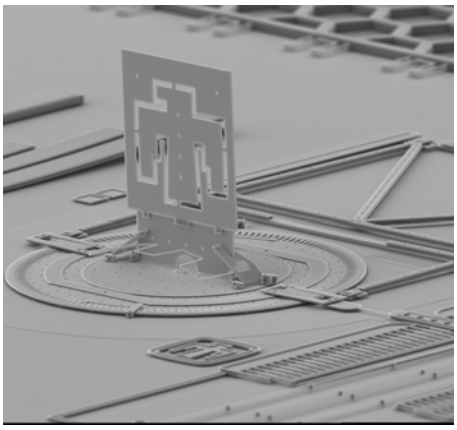

Figure 2.3: Compliant MEMS

2.2.5 Bistable Mechanisms

Reduction of power consumptions in MEMS design can lower operating cost and improve performance thus enabling uses in new application. One way of achieving that goal is by using bistability. A bistable mechanism has two stable positions at the two extremes of its range of motion; it requires low input power because power is only supplied when switching the mechanism from one stable state to the other.

In this thesis, I will focus on the design and analysis of spherical compliant bistable four-bar MEMS with precise and large out of plane displacement.

Chapter 3

Mathematical Background

Several planar compliant bistable mechanisms designs have been demonstrated previously. [16,17,18,19,20]. In this chapter some mathematical concepts implemented in previous work are described that will be useful in the analysis of a spherical compliant bistable four-bar mechanism.

3.1 Planar Mechanisms

This section provides a concise review of the position analysis of a rigid-body mechanism to serve as reference for later comprehension of the concepts behind a spherical four-bar mechanism. Usually, when analyzing a rigid-body mechanism, it is assumed that the elastic deformation of the rigid links of that mechanism is negligible relatively to its general motion. In the following section, the position analysis of a four-bar mechanism is presented [21].

3.1.1 Position Analysis of Planar Four-Bar Mechanism

Many methods have been developed for the position and displacement analysis of a four-bar mechanism. In this paper, we will focus on the analytical

method, specifically a closed-form solution for a four-bar crank-rocker mechanism.

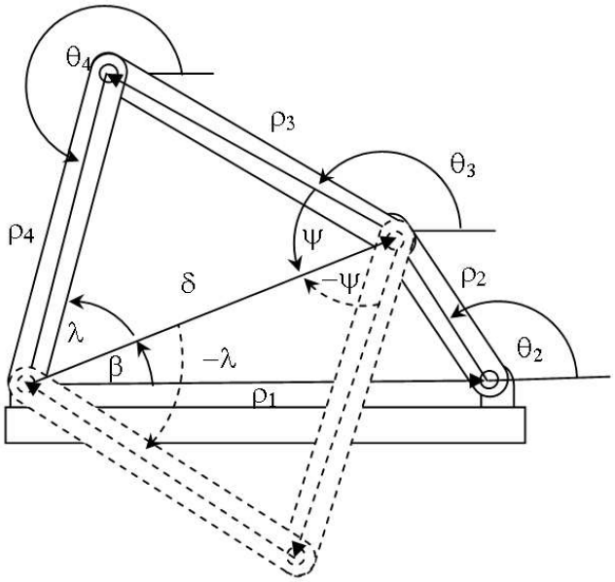

Figure 3.1: Rigid Link Four-Bar Crank-Rocker Mechanism [15]

3.1.1.1 Closed-Form Equations

Consider the four-bar crank-rocker mechanism shown in Figure 1.1. The crank angle, θ_2, is considered to be the input. Using the law of cosines one can find the closed form equations that govern the position of the mechanism. Using the variables defined in Figure 3.1, the closed form equations are:

$$\delta = \sqrt{\rho_1^2 + \rho_2^2 - 2 \cdot |\rho_1| \cdot |\rho_2| \cdot \cos(\pi - \theta_2)} \tag{3.1}$$

$$\beta = \cos^{-1}\left(\frac{\rho_1^2 + \delta^2 - \rho_2^2}{2 \cdot |\rho_1| \cdot \delta} \right) \tag{3.2}$$

$$\psi = \cos^{-1}\left(\frac{\rho_3^2 + \delta^2 - \rho_4^2}{2 \cdot |\rho_3| \cdot \delta}\right) \tag{3.3}$$

$$\lambda = \cos^{-1}\left(\frac{\rho_4^2 + \delta^2 - \rho_3^2}{2 \cdot |\rho_4| \cdot \delta}\right) \tag{3.4}$$

Considering $0 \le \theta_2 \le \pi$, only two possible solutions exist for each of the angles θ_3 and θ_4; the leading and the lagging solutions.

The leading form for each angle is

$$\theta_3 = \beta + \pi - \psi \tag{3.5}$$

$$\theta_4 = \beta + \pi + \lambda \tag{3.6}$$

The lagging form for each angle is

$$\theta_3 = \beta + \pi + \psi \tag{3.7}$$

$$\theta_4 = \beta + \pi - \lambda \tag{3.8}$$

3.1.2 Pseudo-Rigid-Body Model

Numerous methods have been developed to analyze large deflections [22]. The pseudo-rigid-body model (PRBM) provides a simple approach for the analysis of systems that undergo large non-linear elastic deflections [23,24,25,26,27]. This method is very useful when designing compliant mechanisms. Compliant members that undergo large deflections are modeled using rigid-body components with similar force-deflection characteristics [15]. Different types of mechanisms require different models; in this thesis we the small length flexural pivot (SLFP) and the four-bar PRBM. Also, the method of virtual work is a fundamental tool for force deflection behavior of a mechanism.

Thus, it can be used to determine the force-deflection behavior and hence the bistability of a mechanism [18].

3.1.2.1 Small-Length Flexural Pivot

Consider the cantilever beam shown in Figure 3.2 with a force load F at its end. The beam is deflected by an angle θ.

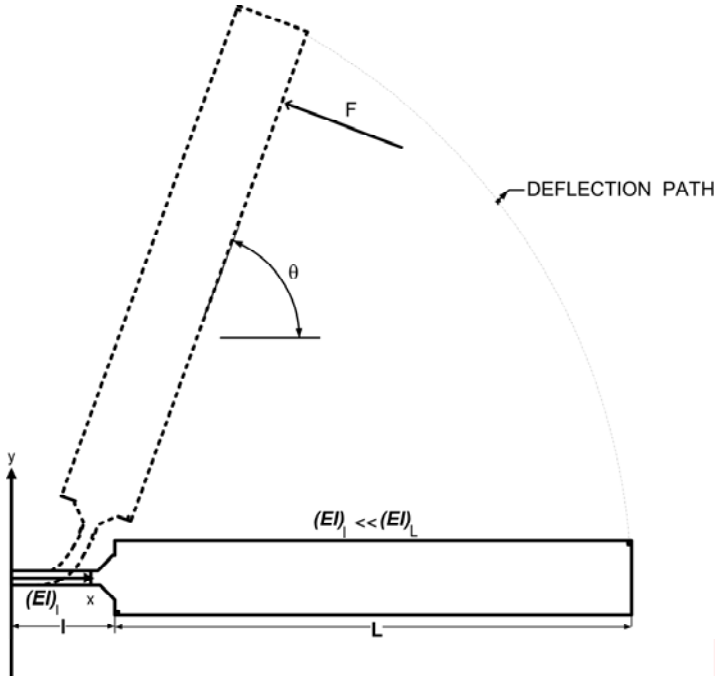

Figure 3.2: Small-Length Flexural Pivot [15]

The beam is composed of two segments: A small flexible segment "l" called small length flexural pivot and a large rigid segment "L". Since "l" is flexible and "L" is rigid, then:

$$(EI)_l << (EI)_L \tag{3.8}$$

Where E the material's Young's modulus and I the second moment of area.

Since the flexible section is a lot shorter than the rigid one, the beam's motion can be modeled as two rigid links connected by a pin joint. The location of the pin joint would be located at the center of the flexural pivot as shown in Figure 3.3.

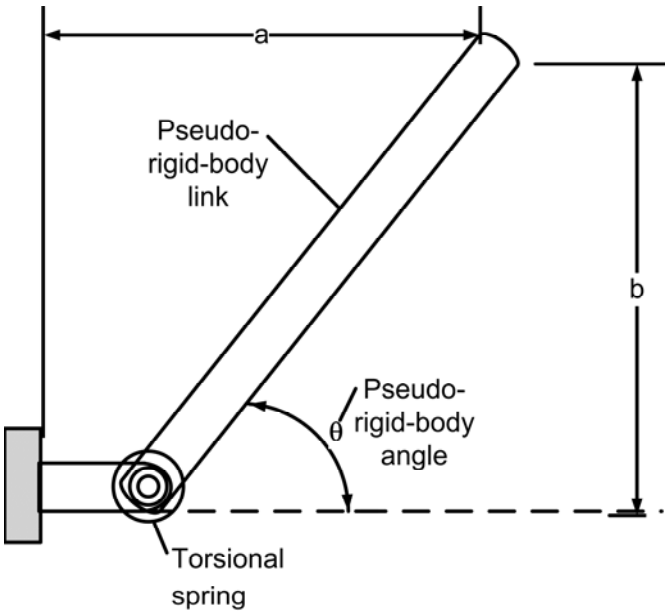

Figure 3.3: Pseudo-Rigid-Body Model

The x and y coordinates of the beam's end are approximated as

$$a = \frac{l}{2} + \left(L + \frac{l}{2} \right) \cdot \cos(\theta) \tag{3.9}$$

And

$$b = \left(L + \frac{l}{2} \right) \cdot \sin(\theta) \tag{3.10}$$

The beams resistance to deflection is modeled using a torsional spring located at the characteristic pivot with constant. The torque required to deflect the spring of an angle θ is:

$$T = K \cdot \theta \tag{3.11}$$

The strain energy stored in the spring is:

$$V = \frac{K}{2} \cdot (\theta - \theta_0)^2 \tag{3.12}$$

Where K is the spring constant and is equal to:

$$K = \frac{(EI)_l}{l} \tag{3.13}$$

Where $(EI)_l$ designated the stiffness of the short compliant section.

3.1.2.2 PRBM Four-Bar Mechanism

A four-bar mechanism with compliant joints can be modeled using the PRBM concept. Figure 3.4 shows a compliant four-bar mechanism with its pseudo-rigid-body model. The compliant joints in Figure 3.4-a) are replaced by torsional springs in Figure 3.4-b).

The energy equations governing a compliant four-bar mechanism can be described using the principle of virtual work. Virtual work is the result of forces acting on system through a virtual displacement. A virtual displacement is an assumed infinitesimal change in the position coordinates of a system such that the constraints remain satisfied. In the case of the PRBM of Figure 3.3, the virtual

work done by the torsional spring can be derived from the derivative of the potential energy, V with respect to a generalized coordinate, $q = \theta$, [15].

$$\delta W = \frac{-dV}{dq} \cdot \delta q \tag{3.14}$$

a)

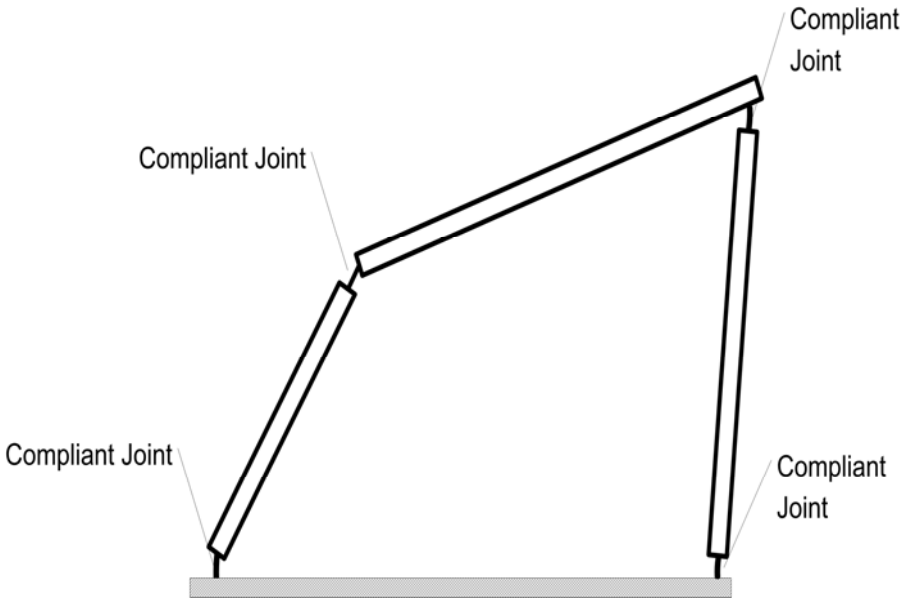

b)

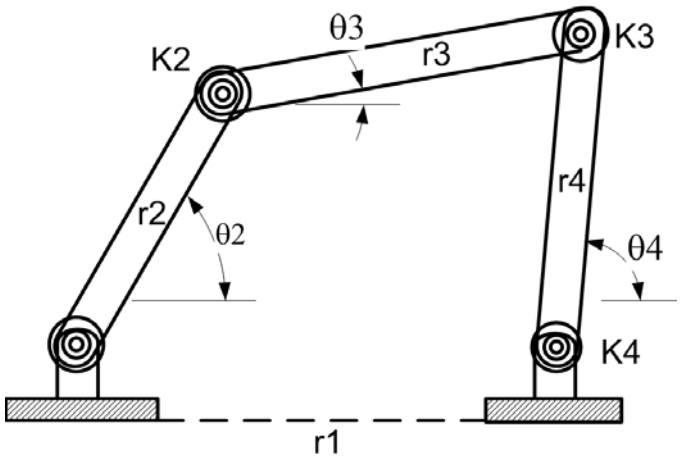

Figure 3.4: Part a) a Compliant Four-Bar Mechanism and Part b) its Pseudo-Rigid Body Model

The total energy stored in the mechanism when an input torque T_{in} is applied to link r_2 is equal to the sum of the potential energy stored in each torsional spring.

$$V_T = \frac{K_1}{2} \cdot (\theta_2)^2 + \frac{K_2}{2} \cdot (\theta_2 - \theta_3)^2 + \frac{K_3}{2} \cdot (\theta_4 - \theta_3)^2 + \frac{K_4}{2} \cdot (\theta_4)^2 \qquad (3.15)$$

The virtual work can be found also by taking the derivative of V_T with respect to θ_2.

$$\delta W = \frac{-dV_T}{dq} \cdot \delta\theta_2 \qquad (3.16)$$

3.1.3 Definition of Bistability

As mentioned Chapter 2, a bistable mechanism is a mechanism that has two stable equilibrium points within its range of motion. A mechanism is considered to be in stable equilibrium if it returns to its equilibrium position after being subject to small forces or disturbances. A mechanism is in an unstable equilibrium when a small force causes the mechanism to change positions, usually to a position of stable equilibrium. According to Lagrange-Dirichlet theorem, an object is in a stable equilibrium when its potential energy is at its local minimum. The bistability concept can be demonstrated with the ball-on-the-hill analogy Figure 3.5. A small impulse applied on to the ball at either ‘A’ or ‘D’ will make oscillate but then it will settle back into its original position. Positions ‘A’ and ‘D’ would then be considered as stable equilibrium positions, locations where

the ball has lowest potential energy. At position ‘B’, the ball is considered to be in unstable equilibrium position because under a small disturbance the ball is going to go to either ‘A’ or ‘D’ positions.

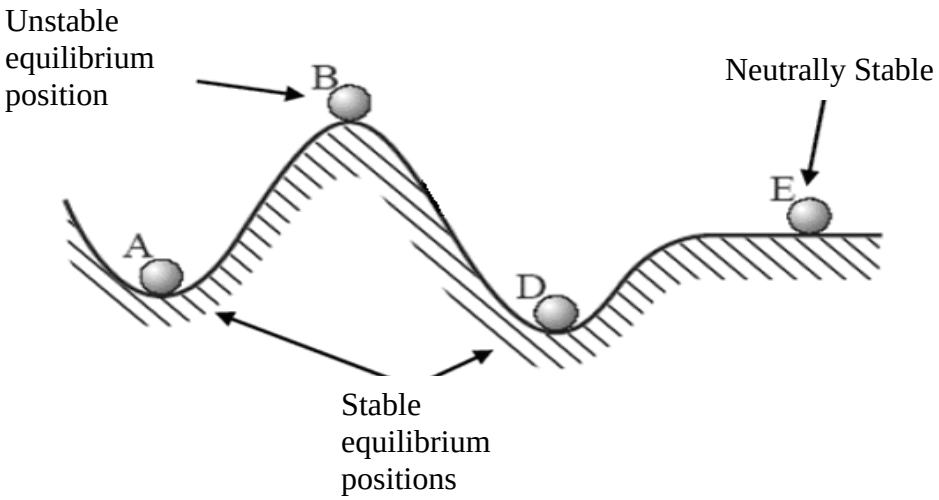

Figure 3.5: Ball-On-The-Hill Analogy for Bistable Mechanisms

3.2 Spherical Mechanisms

A spherical mechanism is a mechanism where the axes of rotation of all its revolute joints intersect at a single point. The shortest distance between this point and any of the mechanism’s joints corresponds to the radius of a sphere that is the virtual workspace of that mechanism. See Figure 3.6.

Figure 3.6: A Spherical Mechanism

This section also provides a brief overview of spherical kinematics to help those with prior knowledge of planar kinematics understand spherical kinematics. Planar kinematics can be related to spherical kinematics by considering a plane as a sphere with infinite radius.

3.2.1 Spherical Trigonometry

The concise analysis of spherical trigonometry given here is based on Spiegel and Liu and develops analogies between spherical trigonometry and plane trigonometry [28]. In planar trigonometry, relationships between straight lines, angles and triangles are obtained on the surface of a flat plane. In spherical trigonometry, the surface is no longer flat but curved according to the surface of the sphere. Thus, geometrical figures are no longer planar but can have mathematically similar properties to their planar counterparts. Circles with the same radius of the sphere that are drawn on the surface of the sphere are called great circles. A great circle displays similar mathematical properties as a straight

line in a plane. Arcs that belong to great circles are called great arcs. Each great circle is contained in a plane that intersects the sphere. The normal to that plane passing through the center of the sphere is the pole of the great circle. The intersection of two great circles of the same sphere form what is called the dihedral angle. A spherical triangle is a triangle formed by the intersection of three great circles with its sides being three great arcs and its angles three dihedral angles. Just as for a planar triangle, there is a Law of Sines and Laws of Cosines that can be applied [29].

In this thesis, upper-case roman letters represent the dihedral angles between the two planes containing intersecting great circles; lower-case roman letters represent great arcs.

Consider the following spherical triangle *ABC* on the sphere shown in Figure 3.4.

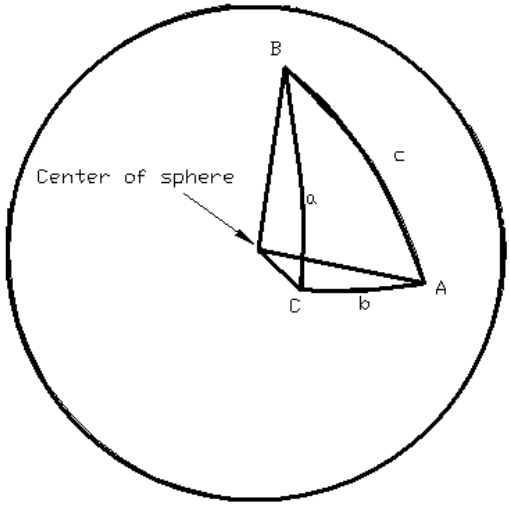

Figure 3.7: A Spherical Triangle with Sides *a, b* and *c* and Dihedral Angles *A, B* and *C.*

In spherical trigonometry there are two Laws of Cosines. The first one relates one dihedral angle and three arcs:

$$\cos a = \cos b \cdot \cos c + \sin b \cdot \sin c \cdot \cos A \tag{3.17}$$

The second Law of Cosines relates one arc with three dihedral angles:

$$\cos A = -\cos B \cdot \cos C + \sin B \cdot \sin C \cdot \cos a \tag{3.18}$$

The spherical Law of Sines relates two arcs and their opposite two dihedral angles:

$$\frac{\sin a}{\sin A} = \frac{\sin b}{\sin B} = \frac{\sin c}{\sin C} \tag{3.19}$$

If one of the dihedral angles of the spherical triangle is equal to $\frac{\pi}{2}$, then the triangle is a right spherical triangle and *Napier's rules* become applicable:

- *The sine of any middle part equals the product of the tangents of the adjacent parts.*
- *The sine of any middle part equals the product of the cosines of the opposite parts.*

There is a simple way to determine which angles are the opposite and which angles are the adjacent angles. Consider the spherical triangle of Figure 3.7 in which the dihedral angle "C" is 90°. The other 5 angles can be drawn into a circle which has been divided into 5 arcs seen in Figure 3.7.

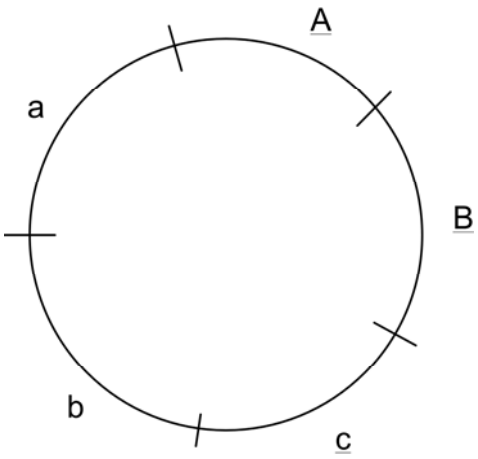

Figure 3.8: Schematic of the Parts of Right Spherical Triangle with Right Angle "C" for Use with Napier's Rules.

In Figure 3.8, $\underline{A}$, $\underline{B}$ and $\underline{c}$ represent the complements of the angles *A*, *B* and *c* of the triangle in Figure 3.6. The complement of an angle *A* is defined by:

$$\underline{A} = 90^0 - A \tag{3.20}$$

The second rule can be used to find *a* if *A* and *c* are known. The Napier circle shows that the two opposite angles to *a* are $\underline{A}$ and $\underline{c}$ while the two adjacent angles are b and $\underline{B}$ Then:

$$\sin(a) = \cos(\underline{A}) \cdot \cos(\underline{c}) = \sin(A) \cdot \sin(c) \tag{3.21}$$

3.2.2 Spherical Four-Bar Mechanism

A spherical four-bar mechanism is a mechanism where the axes of rotation of all pin joints intersect at one point. This point represents the center of the sphere that is the virtual workspace of the mechanism.

The spherical trigonometry properties overviewed in the section above can be utilized to develop the mathematical properties of a spherical four bar mechanism. Consider the spherical four-bar mechanism (SFBM) shown in Figure 3.9 with links r_1, r_2, r_3 and r_4 respectively. The diagonal δ. splits the mechanism into two spherical triangles with their sides being respectively r_1, r_2, δ and r_3, r_4, δ. Note that r_1, r_2, r_3, r_4 and δ. are all great arcs. The dihedral angles of the spherical triangles are represented with lower-case greek letters.

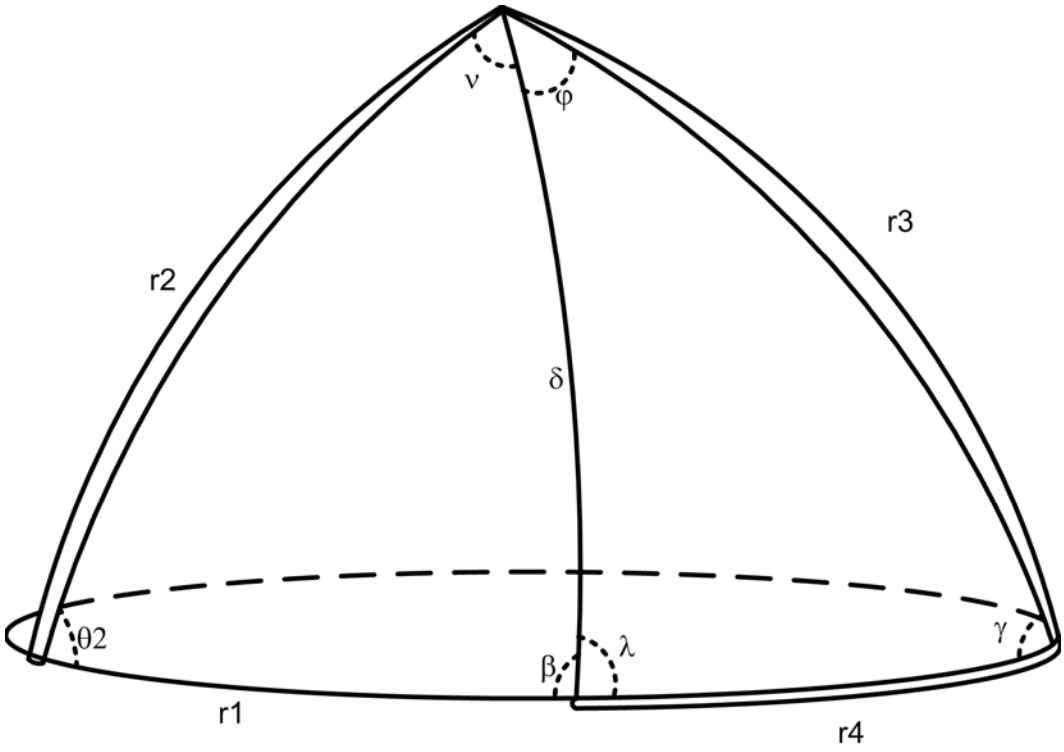

Figure 3.9: Spherical Four-Bar Mechanism with Links r_1, r_2, r_3 and r_4.

By applying the Law of Cosines to each of the two spherical triangles respectively, knowing the link parameters and θ_2, one can solve for all the dihedral angles and the common side, δ.

Applying the spherical Law of Cosines to the spherical triangle on the left hand side in Figure 3.9, we get:

$$\delta = \cos^{-1}\left(\cos(r_1)\cdot\cos(r_2)+\sin(r_1)\cdot\sin(r_2)\cdot\cos(\theta_2)\right) \tag{3.22}$$

$$\beta = \cos^{-1}\left(\frac{\cos(r_2)-\cos(r_1)\cdot\cos(\delta)}{\sin(r_1)\cdot\sin(\delta)}\right) \tag{3.23}$$

$$\upsilon = \cos^{-1}\left(\frac{\cos(r_1)-\cos(r_2)\cdot\cos(\delta)}{\sin(r_2)\cdot\sin(\delta)}\right) \tag{3.24}$$

Applying the spherical Law of Cosines to the spherical triangle on the right hand side in Figure 3.9, we get:

$$\varphi = \cos^{-1}\left(\frac{\cos(r_4)-\cos(r_3)\cdot\cos(\delta)}{\sin(r_4)\cdot\sin(\delta)}\right) \tag{3.25}$$

$$\lambda = \cos^{-1}\left(\frac{\cos(r_3)-\cos(r_4)\cdot\cos(\delta)}{\sin(r_4)\cdot\sin(\delta)}\right) \tag{3.26}$$

$$\gamma = \cos^{-1}\left(\frac{\cos(\delta)-\cos(r_3)\cdot\cos(r_4)}{\sin(r_3)\cdot\sin(r_4)}\right) \tag{3.27}$$

Using the trigonometric identities developed in this chapter, it will be possible to analyze the kinematics of a spherical mechanism in the next chapter.

Chapter 4

Bistability of a Spherical Four-Bar Mechanism

This chapter provides an overview on how the principle of virtual work is used to determine bistability. The position and energy equations of a SFBM are then developed.

4.1 Principle of Virtual Work

To determine the bistability of a spherical compliant mechanism, one way is to apply the principle of virtual work. “The net virtual work of all active forces is zero if and only if an ideal mechanical system is in equilibrium.” In the case where the energy equations and position equations of a mechanism are available the following procedure applies [15].

- *Position analysis.* Obtain the position equations for the mechanism.
- *Energy equations.* Develop the equations that express the energy stored in the springs of the pseudo-rigid body model of the mechanism.
- *First derivative.* Take the first derivative of the energy equations with respect to the generalized coordinate. The resulting equation corresponds to the virtual work equation of the mechanism. It gives

- the relationship between an applied displacement and the reaction moment.
- *Equilibrium positions.* Solve for all values of the generalized coordinate for which the first derivative of the energy equation is zero. These correspond to the equilibrium positions.
- *Stable positions.* Differentiate the energy equation again to find the second derivative of the energy equations with respect to the generalized coordinate. The sign of the result will determine if the equilibrium position is stable or unstable.

4.2 Virtual Work Equations of a Compliant Spherical Four-Bar Mechanism

Consider the spherical mechanism of Figure 3.7 but with four small-length-flexural-pivots replacing the four revolute joints as shown in Figure 4.1-a). The position equations are already developed, see equations 3.22-3.27.The energy equation, similarly to a planar mechanism, can be easily developed using the pseudo-rigid-body model of the compliant spherical four-bar mechanism (CSM) of Figure 4.1-b).

The model has four links r_1, r_2, r_3, r_4 and four torsional springs; acting as four small length flexural pivots; with constants being k_1, k_2, k_3 and k_4. To determine bistability, each possible torsional spring may be examined independently of the others, by choosing its constant, k_i, to be non-zero while setting the other springs' constants equal to zero. Thus a procedure is developed

to determine the bistable behavior due to each spring. The same procedure can then be applied to the other remaining springs.

a)

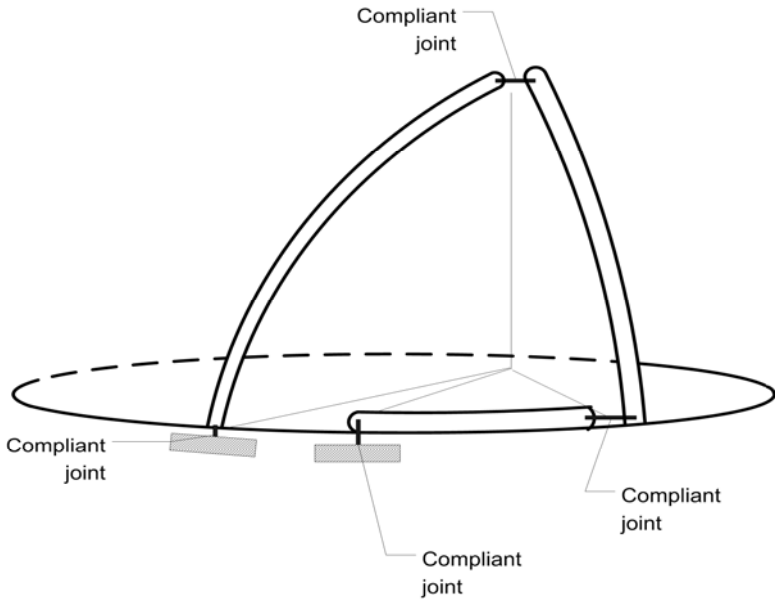

b)

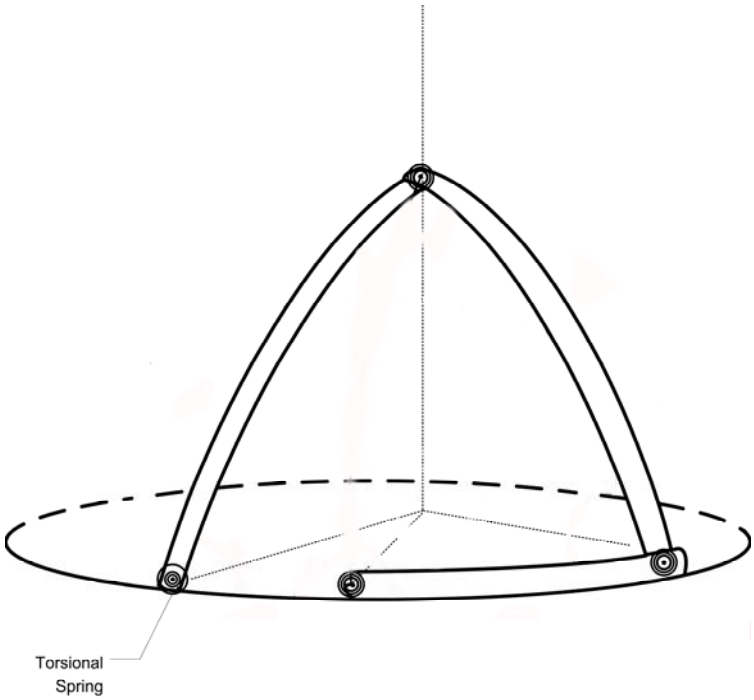

Figure 4.1: a) A Compliant Spherical Four-Bar Mechanism and Its b) PRBM

Recall from Section 3.1.2.2 that a convenient form of virtual work is found from the derivative of the potential energy, *V*, with respect to the generalized coordinate *q*.

$$\delta W = -\frac{dV}{dq}\delta q \tag{4.1}$$

Also, the virtual work δW due to a moment input, M_{in}, and a virtual displacement, $\delta\theta$, is

$$\delta W = M \cdot \delta\theta \tag{4.2}$$

The potential energy stored in any of the four springs is:

$$V = \frac{1}{2} \cdot k \cdot \left(\phi_{final} - \phi_{initial}\right)^2 \tag{4.3}$$

Where $\phi_{initial}$ is the unstressed orientation of the torsional spring.

As mentioned before, stable equilibrium positions can obtained by taking the first derivative of the energy equations with respect to the generalized coordinate and then solving for all values of the generalized coordinate for which the input torque required to maintain a position is zero.

Choosing θ_2 as the generalized coordinate and differentiating with respect to θ_2, the generalized virtual work equation for each torsional spring is:

$$\delta W = -\frac{dV}{d\theta_2}\cdot\delta\theta_2 + M_{in}\cdot\delta\theta_2 = \sum_i -k_i\cdot\left(\phi_{i,final}-\phi_{initial}\right)\frac{d\phi}{d\theta_2}\cdot\delta\theta_2 + M_{in}\cdot\delta\theta_2 \qquad (4.4)$$

M_{in} is the input torque due to a force applied to link r_2. The displacement coordinate associated with M_{in} is the input rotation, $\delta\theta_2$. At equilibrium, the virtual work done δW by the torsional springs is assumed balanced by the work done by the input torque.

Rearranging equation 4.4:

$$M_{in} = -\sum_i k_i\left(\phi_{i,final}-\phi_{i,initial}\right)\frac{d\phi}{d\theta_2} \qquad (4.5\text{-a})$$

Equilibrium positions for a particular torsional spring

$$0 = M_{in} = -k_i\left(\phi_{i,final}-\phi_{i,initial}\right)\frac{d\phi}{d\theta_2} \qquad (4.5\text{-b})$$

The first part of Equation 4.5-b, $-k_i\left(\phi_{i,final}-\phi_{i,initial}\right)$, describes the linear part of the moment due to the torsional spring. It provides only one solution to equation 4.5-b, $\phi_{i,final}=\phi_{i,initial}$,. The second part of Equation 4.5-b, $\frac{d\phi}{d\theta_2}$,the kinematic coefficient, can be non linear and may result in other equilibrium positions when it is equal to zero.

This procedure can be used to evaluate the input moment required at each of the four joints.

4.3 A Simplified Mathematical Model of a Bistable CSM

In the preceding section, a procedure for determining bistability in a general spherical compliant four-bar mechanism was developed. In this section, a specific four-bar-mechanism configuration is considered.

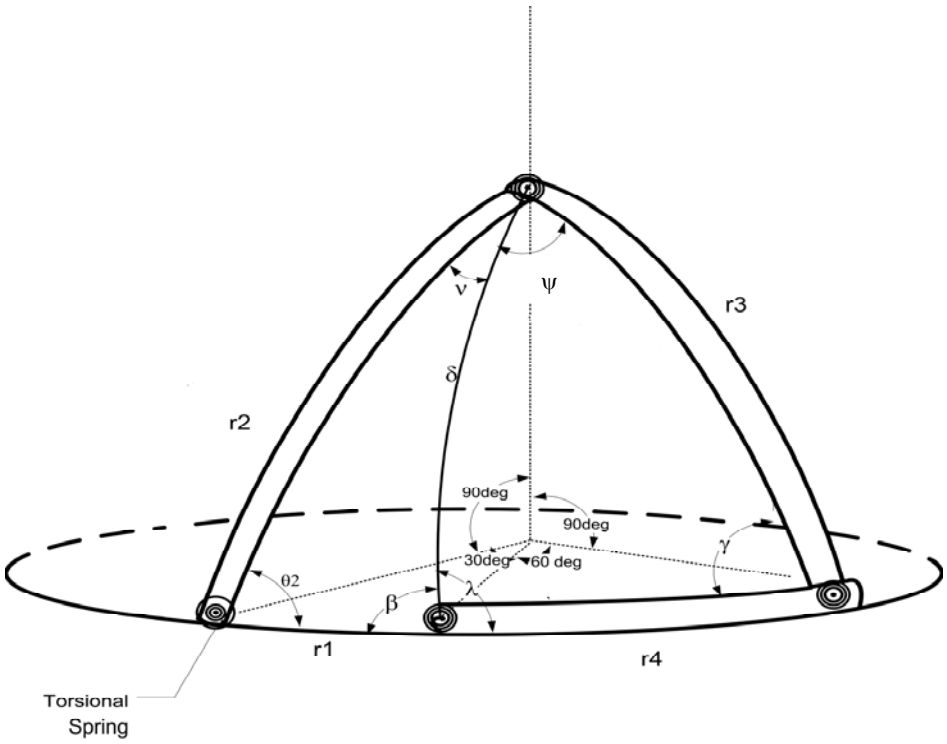

Figure 4.2: PRBM of a Spherical Mechanism with Known Link Lengths

The PRBM of a spherical mechanism which has great arcs as links, with angular measures of r_1=30°, r_2=90°, r_3=90°, r_4=60° is presented in Figure 4.2.

Using these specific angular measurements instead of arc length allows for derivations that are independent of the radius of the particular sphere and simplifies the process for determining bistability.

Recalling equations 4.5-a and 4.5-b with

$$\phi_{12} = \theta_2$$

$$\phi_{23} = \psi + \nu$$

$$\phi_{34} = \gamma$$

$$\phi_{41} = \lambda + \beta$$

An examination of the moment-rotation curve for each joint shows which of the four springs produces two stable positions within the allowable motion of the mechanism.

4.3.1 Joint 1: The Flexural Pivot Connecting Links r_1 and r_2

Using equation 4.5, the moment input required to bend "joint 1" becomes

For $\phi_i = \phi_{12} = \theta_2$

$$M_{in,12} = -k\left(\phi_{12,\,final} - \phi_{12,initial}\right)\frac{d\phi_{12}}{d\theta_2} \tag{4.6}$$

Where $\phi_{12,initial}$ is the undeflected position of the small length flexural pivot and $\frac{d\phi_{12}}{d\theta_2} = 1$. Because $\frac{d\phi_{12}}{d\theta_2} = 1$, the moment-rotation curve is linear. Thus, the elasticity associated with "joint 1" does not produce bistable behavior. One stable position can be seen from that graph and it is located at point *A* of zero rotation of θ_2.

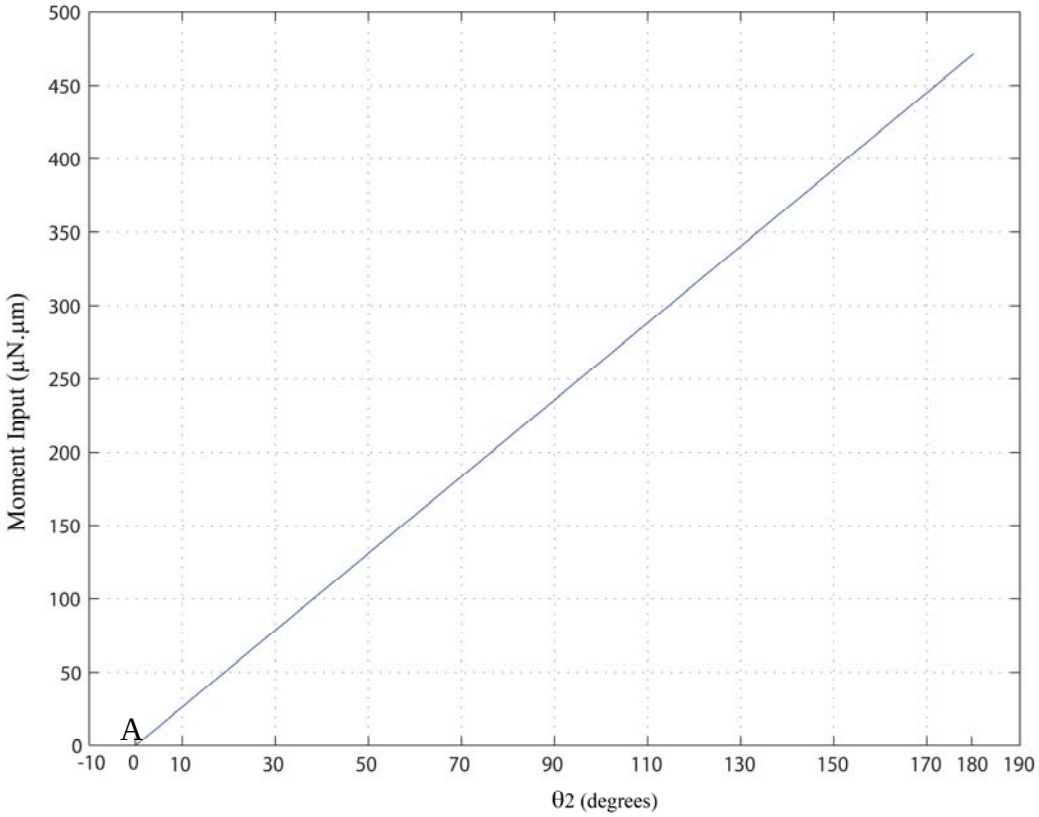

Figure 4.3: Input Moment Required to Hold the Spherical Four-Bar Mechanism in Equilibrium for *Joint 1*

4.3.2 Joint 2: The Flexural Pivot Connecting Links r_2 and r_3

Using equation 4.6 the moment equation is:

For $\phi_i = \phi_{23} = \psi + \nu$

$$M_{in,23} = -k(\phi_{23,\,final} - \phi_{23,initial}) \cdot \frac{d\phi_{34}}{d\theta_2} \tag{4.7}$$

Where

$$\frac{d\phi_{23}}{d\theta_2} = \frac{d\psi}{d\theta_2} + \frac{d\nu}{d\theta_2} \tag{4.8}$$

Using equations 3.24 and 3.25 yields:

$$\frac{d\psi}{d\theta_2} = \frac{d\left(\cos^{-1}\left(\frac{\cos(r_4)-\cos(r_3)\cdot\cos(\delta)}{\sin(r_3)\cdot\sin(\delta)}\right)\right)}{d\theta_2} \tag{4.9}$$

And

$$\frac{d\nu}{d\theta_2} = \frac{d\left(\cos^{-1}\left(\frac{\cos(r_1)-\cos(r_2)\cdot\cos(\delta)}{\sin(r_2)\cdot\sin(\delta)}\right)\right)}{d\theta_2} \tag{4.10}$$

Since r_2=90° and r_3=90° in the case of our mechanism, simplification yields to:

$$\frac{d\psi}{d\theta_2} = \frac{d\left(\cos^{-1}\left(\frac{\cos(r_4)}{\sin(r_3)\cdot\sin(\delta)}\right)\right)}{d\theta_2} \tag{4.11}$$

And

$$\frac{d\nu}{d\theta_2} = \frac{d\left(\cos^{-1}\left(\frac{\cos(r_1)}{\sin(r_2)\cdot\sin(\delta)}\right)\right)}{d\theta_2} \tag{4.12}$$

Differentiating equations 4.11 and 4.12 and substituting back in equation 4.8 yields to:

$$\frac{d\phi_{23}}{d\theta_2} = \left(\frac{-\cos(\lambda)\cdot\sin(r_1)\cdot\sin(\beta)}{\sin(\lambda)} - \frac{-\sin(r_1)\cdot\cos(\beta)}{\sin(\delta)}\right) \tag{4.13}$$

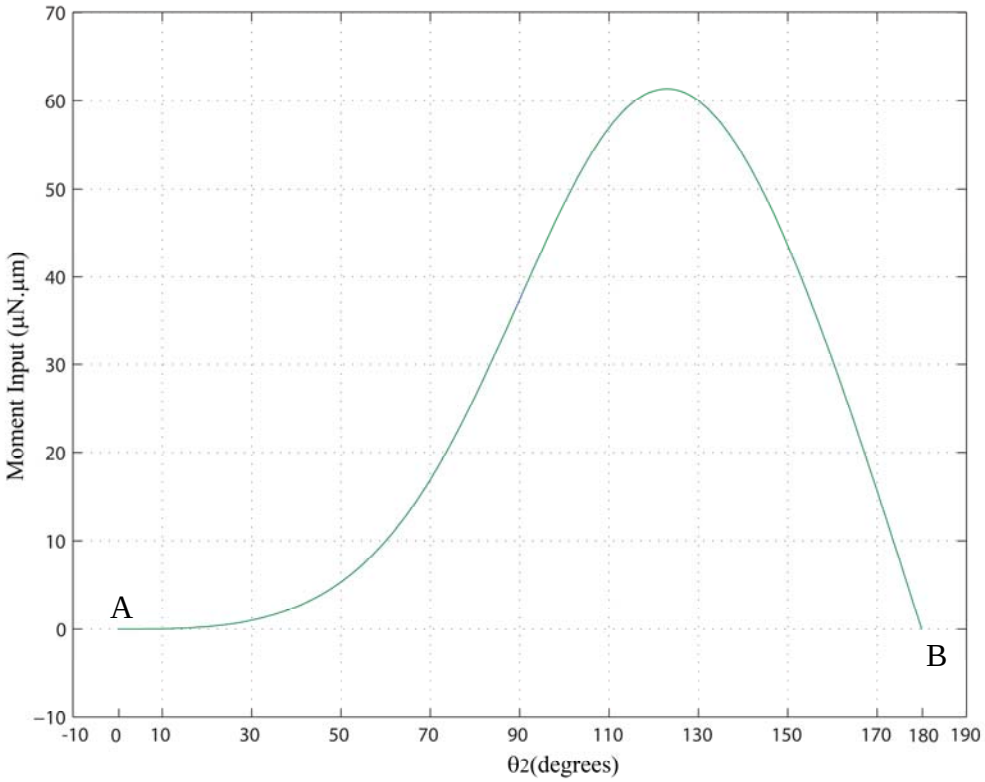

Figure 4.4: Input Moment Required to Hold the Spherical Four-Bar Mechanism in Equilibrium for *Joint 2*

The moment-rotation curve of Figure 4.4 shows that when *joint 2* is the only compliant joint, the mechanism has only two equilibrium positions. The first would be when no input rotation is applied, represented by point *A* in Figure 4.4, and it is a position of stable equilibrium. The second position, a position of unstable equilibrium where the slope of the moment input curve is negative, marked by point *B* in Figure 4.4.

4.3.2 Joint 3: The Flexural Pivot Connecting Links r_3 and r_4

Using equation 4.6 the moment a joint 3 is:

For $\phi_i = \phi_{34} = \gamma$

$$M_{in,34} = -k(\phi_{34} - \phi_{34_0}) \cdot \frac{d\phi_{34}}{d\theta_2} \tag{4.14}$$

Using equation 3.27:

$$\frac{d\phi_{34}}{d\theta_2} = \frac{d\gamma}{d\theta_2} = \frac{d\left(\cos^{-1}\left(\frac{\cos(\delta)-\cos(r_3)\cdot\cos(r_4)}{\sin(r_3)\cdot\sin(r_4)}\right)\right)}{d\theta_2} \tag{4.15}$$

Taking the derivative yields:

$$\frac{d\phi_{34}}{d\theta_2} = \frac{\sin(\delta)\cdot\sin(r_1)\cdot\sin(r_2)\cdot\sin(\theta_2)}{\sqrt{1-U^2}\cdot\sqrt{1-V^2}\cdot\sin(r_3)\cdot\sin(r_4)} \tag{4.16}$$

Where *U*:

$$U = \frac{\cos(\delta)-\cos(r_3)\cdot\cos(r_4)}{\sin(r_3)\cdot\sin(r_4)} \tag{4.17}$$

and *V*:

$$V = \cos(r_1)\cdot\cos(r_2)+\sin(r_1)\cdot\sin(r_2)\cdot\cos(\theta_2) \tag{4.18}$$

Substitution of *U* and *V* in 4.16 and simplifying yields to

$$\frac{d\phi_{34}}{d\theta_2} = \frac{\sin(r_1)\cdot\sin(r_2)\cdot\sin(\theta_2)}{\sin(\gamma)\cdot\sin(r_3)\cdot\sin(r_4)} \tag{4.19}$$

It can be concluded by examining the moment –rotation curve seen in Figure 4.5 that elasticity associated with *joint 3* produces bistable behavior. At 0° rotation, represented by point *A* on the graph of Figure 4.5, the mechanism is in

its first stable equilibrium position. When the input link r_2 is rotated by 90°, the mechanism reaches its non-stable equilibrium position represent by point *B* on the curve of Figure 4.5. The mechanism reaches its second stable equilibrium position, when the input link r_2 is rotated by 180° to point *C* on the graph. Furthermore, the maximum torque levels reached are at points *D* and *E*.

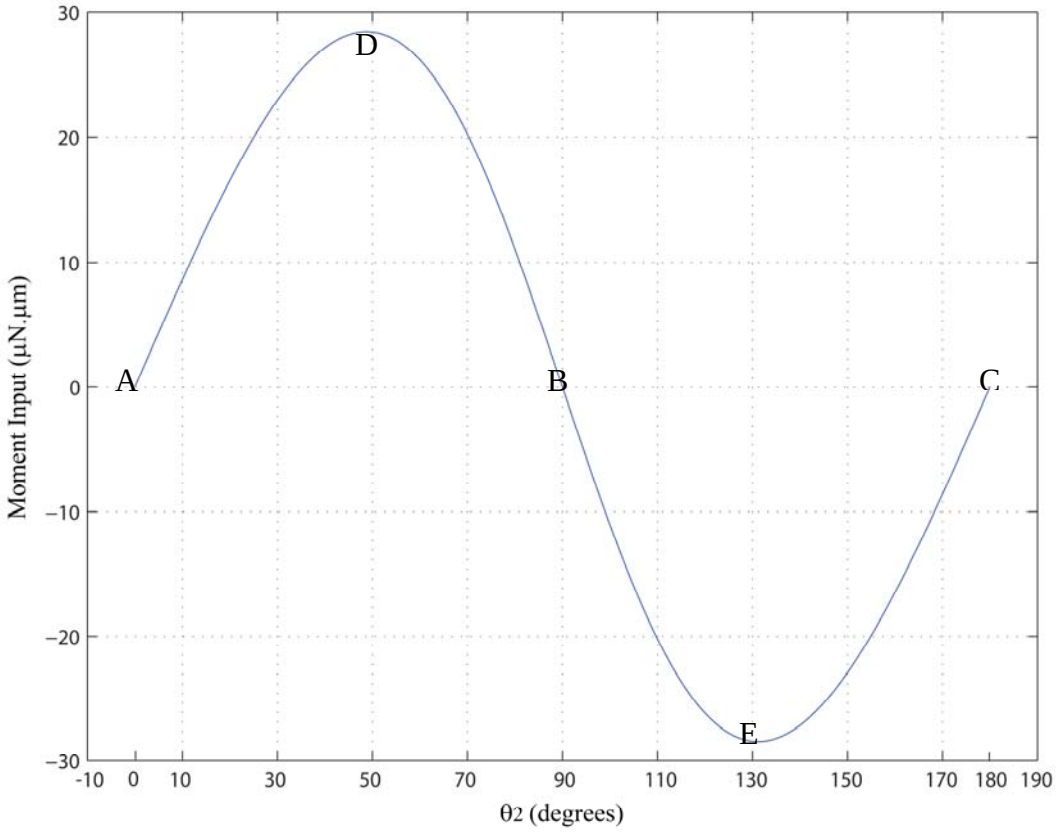

Figure 4.5: Input Moment Required to Hold the Spherical Four-Bar Bechanism in Equilibrium for *Joint 3*

4.3.4 Joint 4: The Flexural Pivot Connecting Links r_4 and r_1

Using equation 3.4 the input moment is:

For $$\phi_i = \phi_{34} = \lambda + \beta$$

$$M_{in,41} = -k(\phi_{41,\,final} - \phi_{41,initial}) \cdot \frac{d\phi_{41}}{d\theta_2} \tag{4.14}$$

Where

$$\frac{d\phi_{41}}{d\theta_2} = \frac{d\lambda}{d\theta_2} + \frac{d\beta}{d\theta_2} \tag{4.15}$$

Using equations 3.23 and 3.26 yields:

$$\frac{d\lambda}{d\theta_2} = \frac{d\left(\cos^{-1}\left(\frac{\cos(r_3) - \cos(r_4)\cdot\cos(\delta)}{\sin(r_3)\cdot\sin(\delta)}\right)\right)}{d\theta_2} \tag{4.16}$$

And

$$\frac{d\beta}{d\theta_2} = \frac{d\left(\cos^{-1}\left(\frac{\cos(r_2) - \cos(r_1)\cdot\cos(\delta)}{\sin(r_1)\cdot\sin(\delta)}\right)\right)}{d\theta_2} \tag{4.17}$$

Since $r_2 = 90°$ and $r_3 = 90°$ in the case of our mechanism, simplification yields:

$$\frac{d\lambda}{d\theta_2} = \frac{d\left(\cos^{-1}\left(\frac{-\cos(r_4)\cdot\cos(\delta)}{\sin(r_3)\cdot\sin(\delta)}\right)\right)}{d\theta_2} \tag{4.18}$$

And

$$\frac{d\beta}{d\theta_2} = \frac{d\left(\cos^{-1}\left(\frac{-\cos(r_1)\cdot\cos(\delta)}{\sin(r_1)\cdot\sin(\delta)}\right)\right)}{d\theta_2} \tag{4.19}$$

Now differentiating equations 4.18 and 4.19 yields:

$$\frac{d\lambda}{d\theta_2} = \frac{\cot(r_4)\cdot\csc^2(\delta)\cdot\sin(r_1)\cdot\sin(r_2)\cdot\sin(\theta_2)}{\sin(\lambda)\cdot\sin(\delta)} \tag{4.20}$$

And

$$\frac{d\beta}{d\theta_2} = \frac{\cot(r_1)\cdot\sin(r_1)\cdot\sin(r_2)\cdot\sin(\theta_2)}{\sin(\beta)\cdot\sin(\delta)} \tag{4.21}$$

Simplifying equations 4.20 and 4.21 and substituting back gives:

$$\frac{d\phi_{41}}{d\theta_2} = \left(\frac{\cos(r_4)\cdot\sin(r_1)\cdot\sin(\beta)}{\sin(r_4)\cdot\sin(\lambda)\cdot\sin(\delta)} + \frac{\cos(r_1)\cdot\sin(r_1)}{\sin(\delta)^2}\right) \tag{4.22}$$

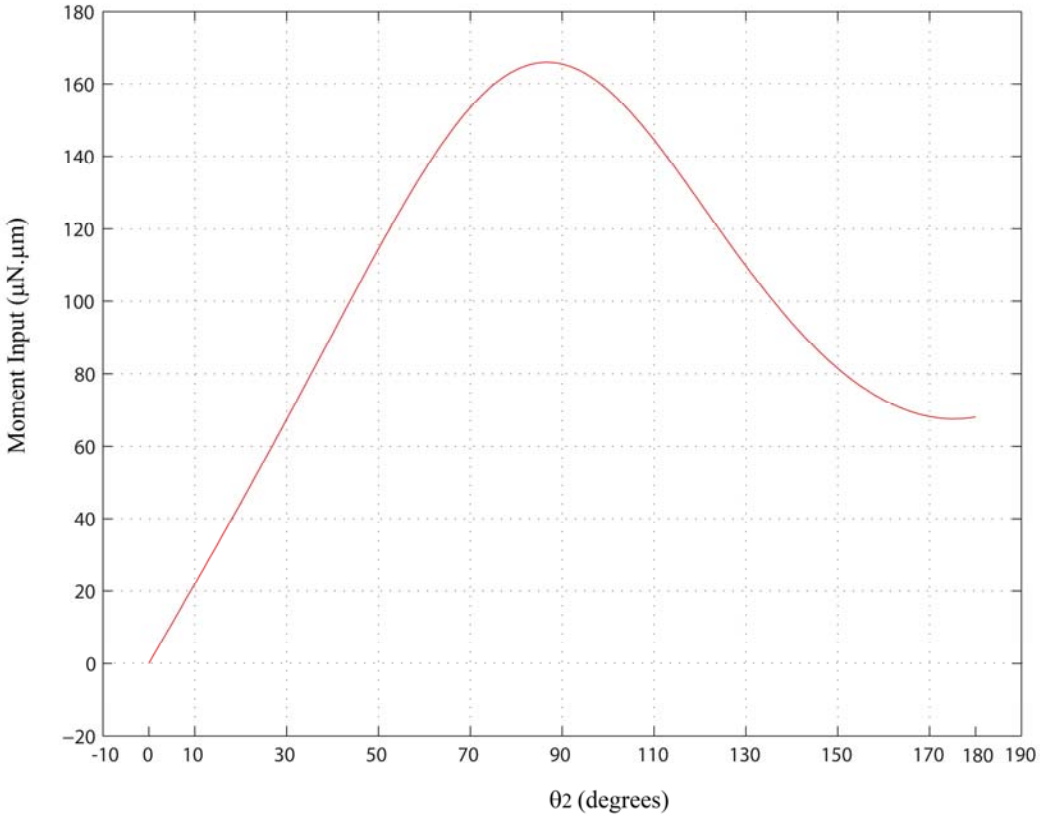

Figure 4.6: Input Moment Required to Hold the Spherical Four-Bar Mechanism in Equilibrium for *Joint 4*

The moment-rotation curve of Figure 4.6 shows that the elasticity associated with *joint 4* produces only one stable position located at the 0° point.

After examining each joint independently, it can be determined that the only compliant joint that allows the mechanism to be bistable is *joint 3.* As for the other joints, they can be compliant but small enough that their *k* constant is very low relatively to k_3 of *joint 3.* The total moment-rotation would then have the similar non-linear shape as the curve of Figure 4.5.

In this chapter, it was demonstrated mathematically that for small length flexural pivots, bistability in a spherical compliant mechanism is possible. In the next chapter, the design and analysis of a bistable spherical compliant four-bar micromechanism is described based on the analysis presented in this chapter.

Chapter 5

A Bistable Spherical Compliant Micromechanism

Micromechanisms with accurate out-off-plane motion and low power consumption are needed and might be useful in several applications [6]. One possible method to achieving that goal is to design a bistable, compliant, spherical mechanism (BSCM).

However, when dealing with micromachining, the design and manufacturing of a bistable, compliant, spherical micromechanism is somewhat challenging because the device is fabricated in plane but its motion is intended to be out-of-plane. In this chapter, the design, fabrication and analysis of a BSCM based on the model developed in Section 4.2 will be presented.

5.1 Fabrication Process

The design of the BSCM followed the design rules set by the micromachining process chosen for fabrication; the Multi-User MEMS Processes (MUMPs). MUMPs is a three-layer polysilicon surface micromachining process. Figure 5.1 shows a cross section of the three-layer polysilicon surface micromachining. This process has the general features of a standard surface micromachining process: (1) polysilicon is used as the structural material, (2) deposited oxide (PSG) is used as the sacrificial layer and silicon nitride

is used as electrical isolation between the polysilicon and the substrate [30].

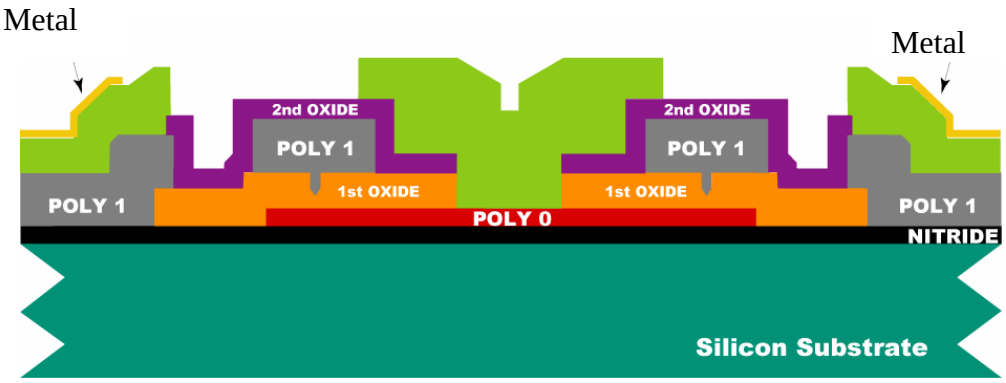

Figure 5.1: Cross Sectional View Showing all 7 Layers of the MUMPs Process [30]

Tables 5.1 lists the material name, thickness and lithography level name of each layer in MUMPS. Table 5.2 shows the minimum feature size for each corresponding layer.

Table 5.1: Layer Names, Thicknesses and Lithography Levels [30]

Material	Material Thickness	CD Tolerances	Lithography Level Name
Nitride	0.6	--	--
Poly 0	0.5	1.800 to 2.200 um Lines	POLY0 (HOLE0)
First Oxide	2.0	1.800 to 2.200 um Spaces 1.700 to 2.300 um Spaces	DIMPLE ANCHOR1
Poly 1	2.0	1.750 to 2.250 um Lines	POLY1 (HOLE1)
Second Oxide	0.75	1.750 to 2.250 um Spaces 1.750 to 2.250 um Spaces	POLY1_POLY2_VIA ANCHOR2
Poly 2	1.5	1.700 to 2.300 um Lines	POLY2 (HOLE2)
Metal	0.5	2.500 to 3.500 um Lines	METAL (HOLEM)

Table 5.2: Minimum Feature Size per Layer of Polysilicon [30]

LEVEL 1	LEVEL 2	MIN FEATURE
POLY0	-	2
	ANCHOR1	
	POLY1	
	ANCHOR2	
	POLY2	
POLY1	-	2
	POLY0	
	ANCHOR1	
	ANCHOR2	
	POLY2	
	DIMPLE	
	POLY1_POLY2_VIA	
POLY2	-	2
	POLY0	
	POLY1	
	VIA	
	ANCHOR2	
	METAL	
HOLEM	HOLE2	
HOLE2	HOLE1	

5.2 Design

The BSCM was designed using computer aided design (CAD) software L-Edit, developed by Tanner Tools. Figure 5.2 represents a simplified sketch of the BSCM. Two different models were designed: *Model 1* where *joint 2* was made compliant and another *Model 2* with *joint 2* was a revolute pin joint. After preliminary testing, *Model 1* was chosen because it was more reliable and easier to design. Figure 5.3 is a scanning electron microscope (SEM) image of the *Model 1* BSCM in its fabricated position. The BSCM has three basic components: Two sliders and a spherical-four bar mechanism with links r_1, r_2, r_3, and r_4 seen in Figures 5.2 and 5.3. r_1 is the ground link, r_2 the input link, r_3 the coupler link and r_4 the follower link. Links r_2 and r_4 are joined to the substrate by a staple hinge that allows 180° rotation. Link r_3 is connected to r_2 and r_4 by compliant joints as

shown in Figure 5.2. The axes of rotation of the four joints intersect at a single point. The sliders act as mechanical actuators and are connected each to the input link r_2, by staple hinges. The mechanism in its fabricated position is shown in Figure 5.3 which is its first stable equilibrium position. By moving the *Raising Slider* to the left, link r_2 will rotate and links r_3 and r_4 will move out-of-plane as shown in Figure 5.5. In order to bring the mechanism back to its original position, *Lowering Slider* would be moved to the right.

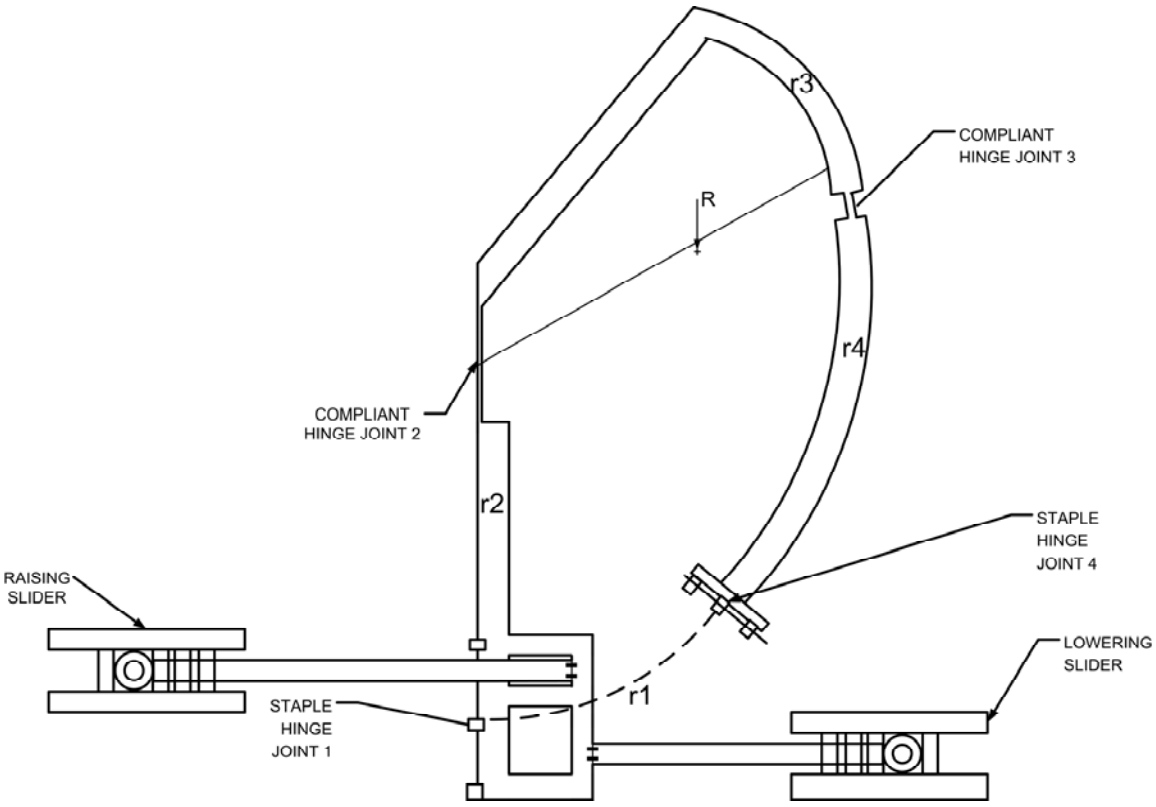

Figure 5.2: BSCM Showing the Nomenclature for the Mechanism

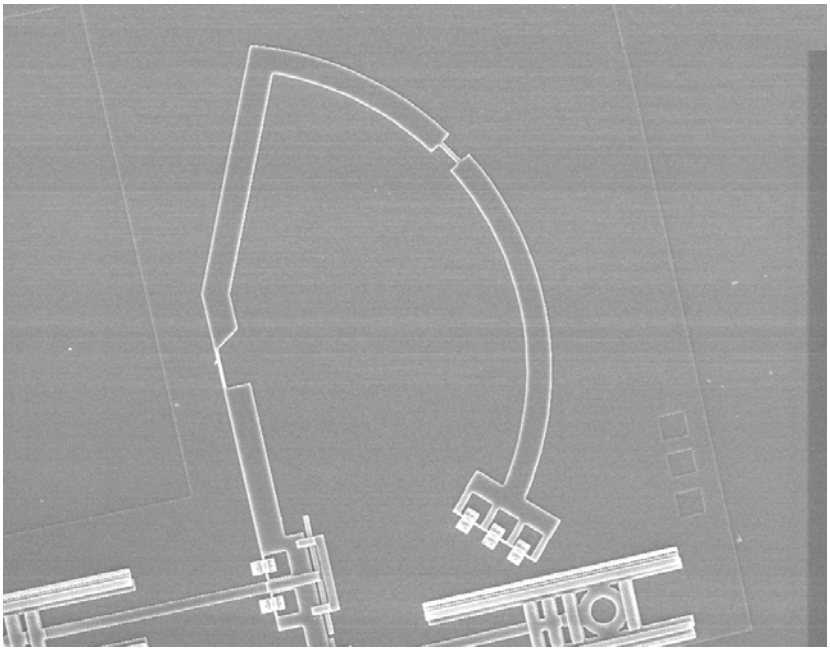

Figure 5.3: Scanning Electron Microscope (SEM) Image of BSCM as Fabricated: First Stable Equilibrium Position

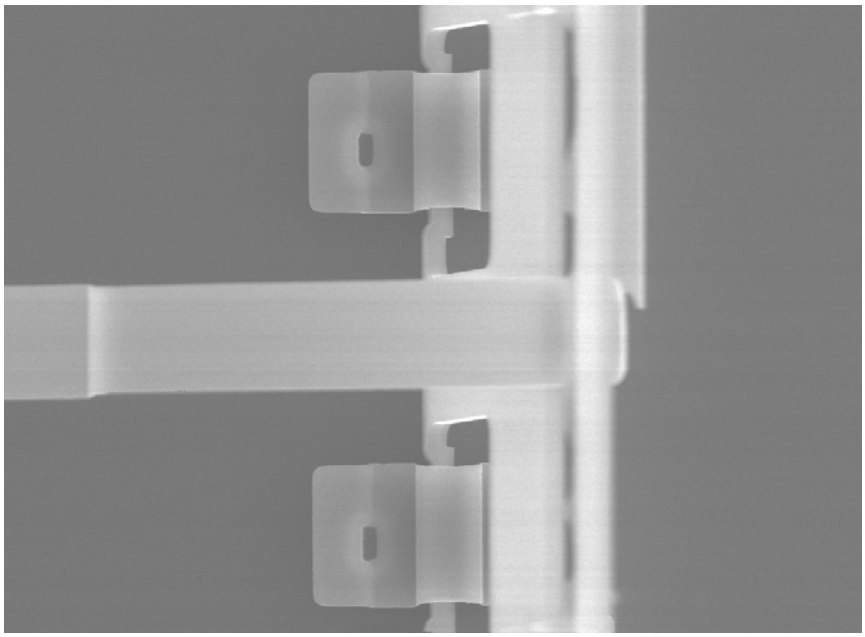

Figure 5.4: SEM Image of the Staple Hinge

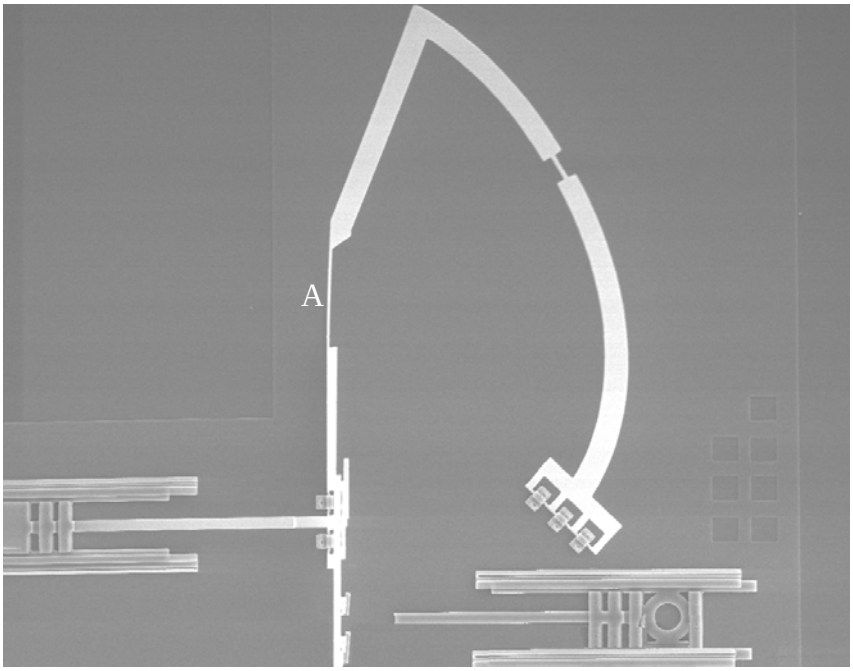

Figure 5.5: SEM Image of the BSCM in an Out-Of-Plane Position

5.3 BSCM Testing

In order to test several configurations of the mechanism, eight models were designed and fabricated. Each model differed from the others in the length of the joint labeled *A* is Figure 5.5, this changes the stiffness *k* of that joint thus affecting the location of the stable equilibrium positions. In order to differentiate the different models on the polysilicon die, each mechanism configuration was marked with a number of squares embedded in the substrate. Testing was done under an optical microscope fitted with a probing station. Two micro-probes with three degrees of freedom (DOF) were placed on the right and left hand side of the prototype. During testing the probes were used to push/pull the slider thus actuating the BSCM.

As mentioned before the BSCM is in its first stable equilibrium position when it is in its “as fabricated position” seen in Figure 5.3.

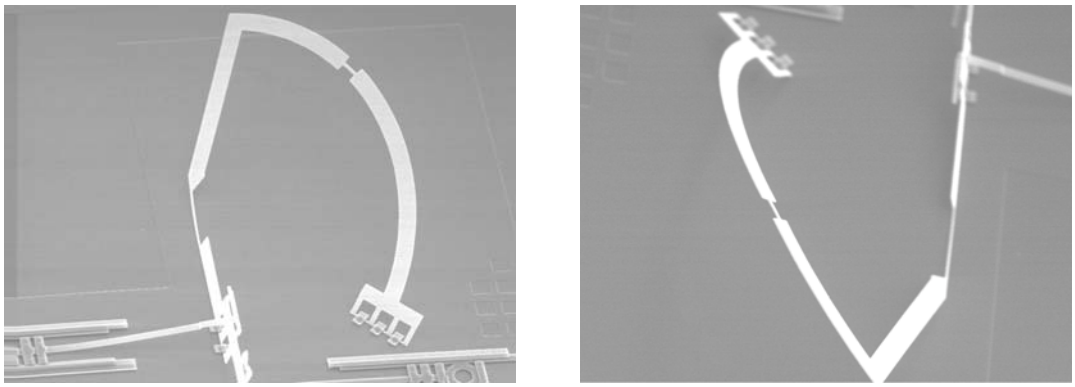

Figure 5.6: SEM Images of BSCM in its Second Stable Equilibrium Position

Figure 5.6 shows the BSCM in its second stable equilibrium position. In this second stable position, the mechanism is in a position in which most of its links are no longer in contact with the substrate (or ground plane). The stability of this second position has been demonstrated experimentally by probing the device at various points along its length and its demonstrating resilience to loading (i.e. always returning to the second stable position).

5.4 Finite-Element Analysis

The BSCM prototype differed in an important way from the elastic mathematical models described in Chapter 4 in that the entire links were more flexible, thus deflections occurred along the length of the mechanism’s links and not just at the short length flexural pivots. The increased flexibility resulted in important qualitative differences in the mechanism’s stability behavior and its

input angle-input torque relation. A Finite-Element Analysis (FEA) (using ANSYS) of the input torque required to hold the mechanism at equilibrium at a given rotation is shown in Figure 5.8.

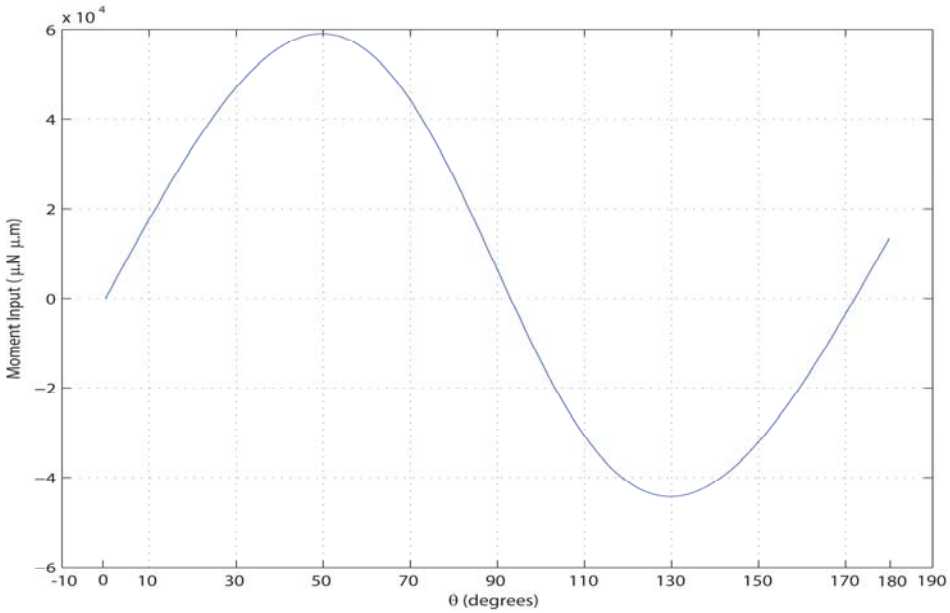

Figure 5.7: Mathematical Model of the Moment-Rotation Relationship for a BSCM with Rigid Links and Short-Length Flexural Pivots

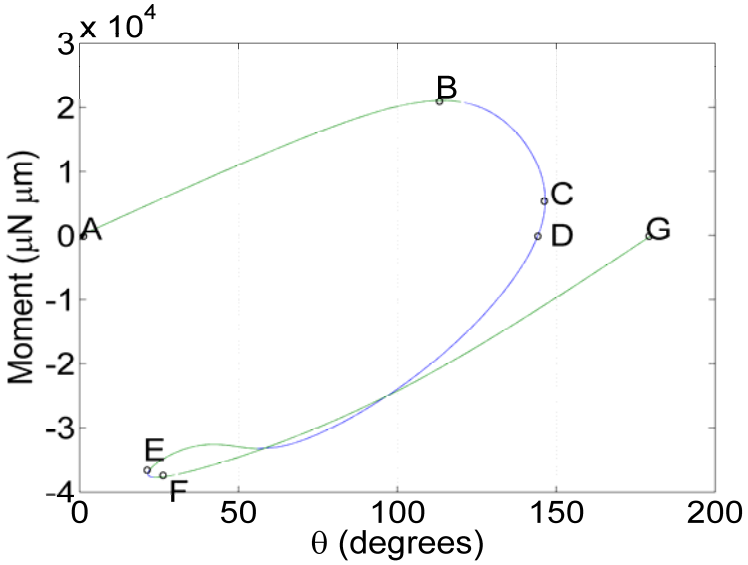

Figure 5.8: Moment-Rotation Relationship from a FEA of the BSCM Prototype

The moment-rotation curve shown in Figure 5.8 shows qualitative differences compared to the curve shown in Figure 5.7. In its initial position, the spherical bistable mechanism is at its first stable equilibrium position, as seen in the mechanism configuration shown in Figure 5.3 and is represented by point *A* in Figure 5.8. The input link is then rotated past 140 degrees to its maximum torque level at point *B*. Then, due to nonlinear deflections in the compliant mechanism, the torque begins to drop off. Intriguingly, both testing and analysis show the existence of a point *C*, past which further rotation of the input link is impossible. At this point, releasing the input causes it to move to a second stable position at *D* rather than back to its original position at *A*. Furthermore, because of the rotation limit at point *C*, it proves very difficult if not impossible to cause the mechanism to return to its original position by rotating the input link. Auxiliary actuation at the second ground point seems to be required to get the mechanism to return to its original configuration. Thus, the region between points *C* and *E* are elastically locked in that the mechanism cannot spontaneously leave this region without auxiliary actuation. Finite Element models show that even very large torques do not cause the mechanism at angle *C* to rotate further. This suggests that the mechanism has potential for high structural strength at or near that position.

Chapter 6

6.1 Conclusions

This paper has discussed the design of an innovative device: A bistable spherical compliant four-bar mechanism. This device offers many valuable features, such as: Two stable positions that require power only when moving from one stable position to the other, precise and repeatable out of plane motion with resistance to small perturbations. The equations for position and input torque have been obtained. The device was fabricated using the MUMPs surface micromachining process. Bistabilty was demonstrated through testing done on a micro-prototype. Compared to the PRBM with small length flexural pivots of the BSCM, Finite-element models of the BSCM indicated important qualitative difference in the mechanism's stability behavior and its input-angle-input moment relation and that may be due to the deflection of the 'rigid' members of the mechanism.

6.2 Recommendations for Future Works

- Results from FEA call for further studies on the BSCM prototype. Stress and force analysis would be helpful in optimizing the BSCM.

- Based on the theory developed in this thesis, prototypes with different parameters could be manufactured and tested for more accurate results.
- In this research, actuation of the BSCM was performed using mechanical micro-probes. Further actuation methods, i.e. Thermomechanical In plane Microactuators (TIM) should be studied and tested.
- Micromachining cost increases with the increase in the number of layers required to build a microprotytpe. For cheaper micromachining, designing a single layer fully compliant BSCM would be helpful.

References

[1] K. J. Gabriel, “Microelectromechanical Systems (MEMS) Tutorial,” *IEEE Test Conference (TC), pp. 432-441, 1998.*

[2] M. Mehregany and M. Huff, “Microelectromechanical Systems," *Proceedings of the IEEE Cornell Conference on Advanced Concepts in High Speed Semiconductor Devices and Circuits, pp. 9-18, 1995.*

[3] C. Lusk, “Ortho-Planar Mechanisms for Microelctromechanical Systems,” Dissertation, Brigham Young University, Provo, UT.

[4] Lam, A.H.F.; Li, W.J.; Yunhui Liu; Ning Xi, "MIDS: micro input devices system using MEMS sensors," *Intelligent Robots and System, 2002.*

[5] Fukushige, T.; Hata, S.; Shimokohbe, A., "A MEMS conical spring actuator array," *Microelectromechanical Systems, Journal of* , vol.14, no.2, pp. 243-253, April 2005.

[6] R. S. Payne, “MEMS commercialization: Ingredients for success," *Proceedings of the IEEE Micro Electro Mechanical Systems (MEMS), pp. 7-10, 2000.*

[7] Texas Instruments, “Digital Light Processors,” http://www.dlp.com/tech/what.aspx, 2007.

[8] J. A. Bradley, “Design of Surface Micromachined Compliant MEMS,” Thesis, Iowa State University, Ames, IA.

[9] J. Parise, L. Howell, and S. Magleby, *“Ortho-planar mechanisms,"* Proceedings of the 2000 ASME Design Engineering Technical Conferences, DETC2000/MECH- 14193, pp. 1-15, 2000.

[10] Ananthasuresh, GK and Howell, Larry L (2005) “Mechanical Design of Compliant Microsystems-A Perspective and Prospects”. *Journal of Mechanical Design* 127(4):pp. 736-738.

[11] Felton, B. “Better robots through clean living”. Intec, May 2001.

[12] R. Cragun and L. L. Howell, “A New Constrained Thermal Expansion Micro-Actuator," *American Society of Mechanical Engineers, Dynamic Systems and Control Division (Publication) DSC*, vol. 66, pp. 365-371, 1998.

[13] C. D. Lott, J. Harb, T. W. McClain, and L. Howell, “Dynamic Modelling of a Surface-Micromachined Linear Thermomechanical Actuator," *Technical Proceedings of the Fourth International Conference on Modeling and Simulation of Microsystems, MSM 2001, Hilton Head Island, South Carolina,* pp. 374-377, 2001.

[14] Howell, L.L. and Midha, A., 1994, "A Method for the Design of Compliant Mechanisms with Small-Length Flexural Pivots," *ASME Journal of Mechanical Design,* Vol. 116, No. 1, pp. 280-290.

[15] L. Howell, Compliant Mechanisms. New York: Wiley-Interscience, 2001

[16] Howell, L.L., Rao, S.S., and Midha, A., 1994, "The Reliability-Based Optimal Design of a Bistable Compliant Mechanism," *ASME Journal of Mechanical Design,* Vol. 116, No.4, pp. 1115-1121.

[17] Jensen, B.D., Howell, L.L., Gunyan, D.B., and Salmon, L.G., 1997, "The Design and Analysis of Compliant MEMS Using the Pseudo-Rigid-Body Model," *Microelectomechanical Systems (MEMS) 1997,* presented at the 1997 ASME International Mechanical Engineering Congress and Exposition, November 16-21, 1997, Dallas, Texas, DSC-Vol. 62, pp. 119-126.

[18] Jensen, B.D., Howell, L.L., and Salmon, L.G., 1998, "Introduction of Two-Link, In-Plane Bistable Compliant MEMS," Proceedings of the 1998 ASME Design Engineering Technical Conferences, DETC98/MECH-5837.

[19] Jensen, B.D., "Identification of Macro- and Micro-Compliant Mechanism Configurations Resulting in Bistable Behavior," M.S. Thesis, Brigham Young University, Provo, Utah.

[20] Jensen, B.D., Howell, L.L., Gunyan, D.B., and Salmon, L.G., 1997, "The Design and Analysis of Compliant MEMS Using the Pseudo-Rigid-Body Model," *Microelectomechanical Systems (MEMS) 1997,* presented at the 1997 ASME International Mechanical Engineering Congress and Exposition, November 16-21, 1997, Dallas, Texas, DSC-Vol. 62, pp. 119-126.

[21] SHIGLEY, J.E. WICKER, J.J. Theory of machines & mechanisms McGraw-Hill, 1980.

[22] B.A. Coulter and R.E. Miller, Numerical analysis of a generalized plane elastica with non-linear material behavior, *Int J Numer Meth Eng* 26 1988, pp. 617–630.

[23] Howell, L.L. and Midha, A., 1994, "A Method for the Design of Compliant Mechanisms with Small-Length Flexural Pivots," *ASME Journal of Mechanical Design,* Vol. 116, No. 1, pp. 280-290.

[24] Howell, L.L., and Midha, A., 1996, "A Loop-Closure Theory for the Analysis and Synthesis of Compliant Mechanisms," *ASME Journal of Mechanical Design,* Vol. 118, No. 1, pp. 121-125.

[25] Salmon, L.G., Gunyan, D.B., Derderian, J.M., Opdahl, P.G., and Howell, L.L., 1996, "Use of the Pseudo-Rigid Body Model to Simplify the Description of Compliant Micro-Mechanisms," *1996 IEEE Solid-State and Actuator Workshop*, Hilton Head Island, SC, pp. 136-139.

[26] Salamon, B.A., and Midha, A., 1992, "An Introduction to Mechanical Advantage in Compliant Mechanisms," *Advances in Design Automation,* (Ed.: D.A. Hoeltzel), DE-Vol 44-2, 18th ASME Design Automation Conference, pp. 47-51.

[27] Howell, L.L., Midha, A., and Norton, T.W., 1996, "Evaluation of Equivalent Spring Stiffness for Use in a Pseudo-Rigid-Body Model of Large-Deflection Compliant Mechanisms," *ASME Journal of Mechanical Design,* Vol. 118, No. 1, pp. 126-131.

[28] M. R. Spiegel and J. Liu, Schaum's Outlines: Mathematical Handbook of Formulas and Tables. New York, NY: McGraw-Hill, 1999.

[29] D. W. Henderson, Experiencing Geometry: In Euclidean, Spherical, and Hyperbolic Spaces, 2nd Edition. Upper Saddle River, NJ: Prentice Hall, 2001.

[30] D. Koester, R. Mahadevan, B. Hardy, and K. Markus, MUMPs Design Handbook.Research Triangle Park, NC: Cronos Integrated Microsystems, 2001.

Appendices

Appendix A: ANSYS Batch Files

The following files are test files written in notepad. They are Batch files used by ANSYS to run FEA and determine the moment input on the micro-prototype. Each file contains different prototype dimensions.

Batch File 1:

```
!************************************
/CONFIG,NRES,1000000
!/CWD,'C:\Documents and Settings\aleon2\Desktop\Work'

!************************************


!****************************************
!******* Set Up Model Variables *********
!****************************************


!*DO,asp, .1,.7,.3
!asp =.1
!aspect    = 10*asp
!*DO,arclength,1,120,1
!arclength=10

/title,3D Beam Non-linear Deflection
/PREP7
!LCLEAR, ALL
!LDELE, ALL
!KDELE, ALL

R=313.38  ! length in micrometers
PI=acos(-1.)
h1=2
b1=20
```

Appendix A (Continued)

```
b2=5
h2=2

b3=27.6
h3=2

!********** Area properties **************

A1 = h1*b1

Iy1= 1/12*b1*h1*h1*h1
Iz1= 1/12*h1*b1*b1*b1

E1= 169E3  ! Young's modulus in MPa, Force will be micro Newtons

!***********************************

A2=  h2*b2

Iz2= 1/12*h2*b2*b2*b2
Iy2= 1/12*b2*h2*h2*h2

E2= 169e3

!***********************************

A3=  h3*b3

Iz3= 1/12*h3*b3*b3*b3
Iy3= 1/12*b3*h3*h3*h3

E3= 169e3


!********** Declare an element type: Beam 4 (3D Elastic) *********

ET,1,BEAM4
KEYOPT,1,2,1
KEYOPT,1,6,1
```

Appendix A (Continued)

```
R,1,A1,Iy1,Iz1,h1,b1, ,          !******Check on the assumptions being made ******

R,2,A2,Iy2,Iz2,h2,b2, ,

R,3,A3,Iy3,Iz3,h3,b3, ,

MPTEMP,1,0
MPDATA,EX,1,,E1
MPDATA,PRXY,1,,0.35              ! Material properties for material 1 and 2


MPTEMP,1,0
MPDATA,EX,2,,E2
MPDATA,PRXY,2,,0.35

MPTEMP,1,0
MPDATA,EX,3,,E3
MPDATA,PRXY,3,,0.35

!***********************************


!********** Create Keypoints 1 throug 7: K(Point #, X-Coord, Y-Coord, Z-Coord)
          *********

K,1,0,0,0,
K,2,0,-225,0,
K,3,0,-50,0,
K,4,0,50,0,
K,5,R*cos(PI/180*72),R*SIN(PI/180*72),0,
K,6,R*cos(PI/180*33),R*sin(PI/180*33),0,
K,7,R*cos(PI/180*29),R*sin(PI/180*29),0,
K,8,R*cos(PI/180*44),-R*sin(PI/180*44),0,


!********* Create Beam using Lines and Arcs and divide into segments *********

LSTR,      2,      3
LSTR,      4,      5
LSTR,      3,      4              ! Draws lines connecting keypoints 1 through 7
LSTR,      6,      7
```

Appendix A (Continued)

```
LARC,5,6,1,R,                    ! Defines a circular arc
LARC,7,8,1,R,
LESIZE,ALL,,,15                  ! Specifies the divisions and spacing ratio on
        unmeshed lines, *****Try making 32 smaller


!********** MESH **********

real,3              ! Use real constant set 3
type,1              ! Use element type 1
mat,3               ! use material property set 3

LMESH,1,2           ! mesh lines 1-2

real,2              ! Use real constant set 2
type,1              ! Use element type 1
mat,2               ! use material property set 2
LMESH,3,4           ! mesh line 3-4

real,1              ! Use real constant set 1
type,1              ! Use element type 1
mat,1               ! use material property set 1
LMESH,5,6           ! mesh line 5-6


!******* Get Node Numbers at chosen keypoints *******


ksel,s,kp,,2
nslk,s
*get,nkp2,node,0,num,max          ! Retrieves a value and stores it as a scalar
        parameter or part of an array parameter**********
nsel,all
ksel,all

ksel,s,kp,,3
nslk,s
*get,nkp3,node,0,num,max
nsel,all
ksel,all
ksel,s,kp,,4
nslk,s
```

Appendix A (Continued)

```
*get,nkp4,node,0,num,max
nsel,all
ksel,all

ksel,s,kp,,5
nslk,s
*get,nkp5,node,0,num,max
nsel,all
ksel,all

ksel,s,kp,,6
nslk,s
*get,nkp6,node,0,num,max


nsel,all
ksel,all

ksel,s,kp,,7
nslk,s
*get,nkp7,node,0,num,max
nsel,all
ksel,all


ksel,s,kp,,8
nslk,s
*get,nkp8,node,0,num,max
nsel,all
ksel,all
FINISH

!*************************************************************
!********************** SOLUTION ***************************
!*************************************************************
/SOL
ANTYPE,0                    ! Specifies the analysis type and restart status and
        "0" means that it Performs a static analysis. Valid for all degrees of
        freedom

NLGEOM,1                    ! Includes large-deflection effects in a static or full
        transient analysis
```

Appendix A (Continued)

```
!AUTOTS, ON
!CNVTOL,U,,0.000001,,0
!CNVTOL,F,,0.0001,,0              ! Sets convergence values for nonlinear
        analyses

!***********************************

DK,2, ,0, , , ,UX,UY,UZ,ROTX,ROTZ,  ! Boundary conditions on keypoint 2
DK,3, ,0, , , ,UX,UY,UZ,ROTX,ROTZ,  ! Boundary conditions on keypoint 2

DK,8, ,0, , , ,UX,UY,UZ,ROTZ,
LOCAL,11,CART,0,0,0,-44,0,0,
CSYS,11
DK,8,ROTY,0


CSYS,0

!***********************************
*DIM,my1,TABLE,10000

lsnum =0

*DO,step,1,120,1
        theta=-1*step
        DK,2,ROTY,theta*PI/180
        lsnum=lsnum+1
        LSWRITE,lsnum
*ENDDO
stop1 = lsnum


!Arclen,On
!*DO,step,143,146,.01
        !theta = -1*step
        !DK,2,ROTY,theta*PI/180
        !lsnum=lsnum+1
        !LSWRITE,lsnum
!*ENDDO

DKDELE,2,ROTY
```

Appendix A (Continued)

```
*DO,step,-20750,33250,250                    !Maximum Moment Value -
        2.1065e+004
        mmy1 = step*1
        FK,2,MY,mmy1

      lsnum=lsnum+1
      *set,MY1(lsnum),step*1

        LSWRITE,lsnum
*ENDDO

FKDELE,2,my

*DO,step,-56,-22,1
        theta=1*step
        DK,2,ROTY,theta*PI/180
        lsnum=lsnum+1


LSWRITE,lsnum
*ENDDO

DKDELE,2,ROTY

*DO,step,36500,37725,25                      !Maximum Moment Value -
        2.1065e+004
        mmy1 = step*1
        FK,2,MY,mmy1

      lsnum=lsnum+1
      *set,MY1(lsnum),step*1

        LSWRITE,lsnum
*ENDDO

FKDELE,2,my
*DO,step,-23.3,-24,-.1
        theta=1*step
        DK,2,ROTY,theta*PI/180
        lsnum=lsnum+1
        LSWRITE,lsnum
*ENDDO
```

Appendix A (Continued)

```
*DO,step,-24,-30,-1
        theta=1*step
        DK,2,ROTY,theta*PI/180
        lsnum=lsnum+1
        LSWRITE,lsnum
*ENDDO

*DO,step,-30,-180,-1
        theta=1*step
        DK,2,ROTY,theta*PI/180
        lsnum=lsnum+1
        LSWRITE,lsnum
*ENDDO

*Do,nn,1,lsnum

LSSOLVE,nn


/output,progress,txt,,append
*VWRITE,nn              ! Writes data to a file in a formatted sequence
%16.8G

/output
*enddo


/STATUS,SOLU
FINISH

!*****************************
!******* GET RESULTS *********
!*****************************
loadSteps=lsnum
/POST1
*DIM,rotY2,TABLE,loadSteps
*DIM,disX3,TABLE,loadSteps
*DIM,disY3,TABLE,loadSteps
*DIM,disZ3,TABLE,loadSteps
*DIM,disX5,TABLE,loadSteps
*DIM,disY5,TABLE,loadSteps
*DIM,disZ5,TABLE,loadSteps
```

Appendix A (Continued)

```
!*DIM,fx1,TABLE,loadSteps
!*DIM,fy1,TABLE,loadSteps
!*DIM,fz1,TABLE,loadSteps
!*DIM,mx1,TABLE,loadSteps
!*DIM,mz1,TABLE,loadSteps
*DIM,momy2,TABLE,loadSteps

!*DIM,fx2,TABLE,loadSteps
!*DIM,fy2,TABLE,loadSteps
!*DIM,fz2,TABLE,loadSteps
!*DIM,mx2,TABLE,loadSteps
!*DIM,my2,TABLE,loadSteps
!*DIM,mz2,TABLE,loadSteps

!*DIM,fx3,TABLE,loadSteps
!*DIM,fy3,TABLE,loadSteps
!*DIM,fz3,TABLE,loadSteps
!*DIM,mx3,TABLE,loadSteps
!*DIM,my3,TABLE,loadSteps
!*DIM,mz3,TABLE,loadSteps


!*DIM,fx5,TABLE,loadSteps
!*DIM,fy5,TABLE,loadSteps
!*DIM,fz5,TABLE,loadSteps
!*DIM,mx5,TABLE,loadSteps
!*DIM,my5,TABLE,loadSteps
!*DIM,mz5,TABLE,loadSteps

*Do,nn,1,lsnum
set,nn
*GET,roty,Node,nkp2,ROT,Y
*SET,rotY2(nn),roty
*GET,my2,Node,nkp2,RF,MY
*SET,MOMY2(nn),my2

*ENDDO

/output,output_arc%arclength%_asp%aspect%,txt,,
*MSG,INFO,'t','w','R','E','arclength'          ! Writes an output message via the
          ANSYS message subroutine
%-8C %-8C %-8C %-8C %-8C
```

Appendix A (Continued)

```
*VWRITE,h2,b2,R,E2,arclength                ! Writes data to a file in a formatted
        sequence
%16.8G %-16.8G %-16.8G %-16.8G %-16.8G

*MSG,INFO,'roty2','my1','my2'
%-8C %-8C


*VWRITE,rotY2(1),MY1(1),MOMY2(1)
%16.8G %-16.8G %-16.8G
/output


FINISH

!*ENDDO
!*ENDDO
```

Batch File 2

```
!************************************
/CONFIG,NRES,1000000
!/CWD,'C:\Documents and Settings\aleon2\Desktop\Work'

!************************************



!****************************************
!******* Set Up Model Variables *********
!****************************************



!*DO,asp, .1,.7,.3
!asp =.1
!aspect    = 10*asp
!*DO,arclength,1,120,1
!arclength=10

/title,3D Beam Non-linear Deflection
```

Appendix A (Continued)

```
/PREP7
!LCLEAR, ALL
!LDELE, ALL
!KDELE, ALL

R=313.38  ! length in micrometers
PI=acos(-1.)
h1=2
b1=25

b2=5
h2=2

b3=27.6
h3=2


b4=3.5


h4=2
!********** Area properties **************

A1 = h1*b1

Iy1= 1/12*b1*h1*h1*h1
Iz1= 1/12*h1*b1*b1*b1

E1= 169E3  ! Young's modulus in MPa, Force will be micro Newtons

!************************************

A2=  h2*b2

Iz2= 1/12*h2*b2*b2*b2
Iy2= 1/12*b2*h2*h2*h2

E2= 169e3

!************************************

A3=  h3*b3
```

Appendix A (Continued)

```
Iz3= 1/12*h3*b3*b3*b3
Iy3= 1/12*b3*h3*h3*h3

E3= 169e3
!***********************************

A4=  h4*b4

Iz4= 1/12*h4*b4*b4*b4
Iy4= 1/12*b4*h4*h4*h4

E4= 169e3

!***********************************

!********** Declare an element type: Beam 4 (3D Elastic) *********

ET,1,BEAM4
KEYOPT,1,2,1
KEYOPT,1,6,1



!********** Set Real Constants and Material Properties *********

R,1,A1,Iy1,Iz1,h1,b1, ,          !******Check on the assumptions being made ******

R,2,A2,Iy2,Iz2,h2,b2, ,

R,3,A3,Iy3,Iz3,h3,b3, ,

R,4,A4,Iy4,Iz4,h4,b4, ,

MPTEMP,1,0
MPDATA,EX,1,,E1
MPDATA,PRXY,1,,0.35              ! Material properties for material 1 and 2

MPTEMP,1,0
MPDATA,EX,2,,E2
MPDATA,PRXY,2,,0.35
MPTEMP,1,0
MPDATA,EX,3,,E3
```

Appendix A (Continued)

```
MPDATA,PRXY,3,,0.35

MPTEMP,1,0
MPDATA,EX,4,,E4
MPDATA,PRXY,4,,0.35

!************************************


!********** Create Keypoints 1 throug 7: K(Point #, X-Coord, Y-Coord, Z-Coord)
        *********

K,1,0,0,0,
K,2,0,-225,0,
K,3,0,-50,0,
K,4,0,50,0,
K,5,R*cos(PI/180*72),R*SIN(PI/180*72),0,
K,6,R*cos(PI/180*33),R*sin(PI/180*33),0,
K,7,R*cos(PI/180*29),R*sin(PI/180*29),0,
K,8,R*cos(PI/180*44),-R*sin(PI/180*44),0,


!********* Create Beam using Lines and Arcs and divide into segments *********

LSTR,      2,      3
LSTR,      4,      5
LSTR,      3,      4              ! Draws lines connecting keypoints 1 through 7
LSTR,      6,      7
LARC,5,6,1,R,                     ! Defines a circular arc
LARC,7,8,1,R,
LESIZE,ALL,,,15                   ! Specifies the divisions and spacing ratio on
        unmeshed lines, *****Try making 32 smaller


!********** MESH **********

real,3                ! Use real constant set 3
type,1                ! Use element type 1
mat,3                 ! use material property set 3
LMESH,1,2             ! mesh lines 1-2
```

Appendix A (Continued)

```
type,1                  ! Use element type 1
mat,2                   ! use material property set 2
LMESH,4                 ! mesh line 4

real,4                  ! Use real constant set 4
LMESH,3                         ! mesh line 3

real,1                  ! Use real constant set 1
type,1                  ! Use element type 1
mat,1                   ! use material property set 1
LMESH,5,6               ! mesh line 5-6



!******* Get Node Numbers at chosen keypoints *******


ksel,s,kp,,2
nslk,s
*get,nkp2,node,0,num,max            ! Retrieves a value and stores it as a scalar
        parameter or part of an array parameter***********
nsel,all
ksel,all


ksel,s,kp,,3
nslk,s
*get,nkp3,node,0,num,max
nsel,all
ksel,all

ksel,s,kp,,4
nslk,s
*get,nkp4,node,0,num,max
nsel,all
ksel,all

ksel,s,kp,,5
nslk,s
*get,nkp5,node,0,num,max
nsel,all
ksel,all
```

Appendix A (Continued)

```
ksel,s,kp,,6
nslk,s
*get,nkp6,node,0,num,max
nsel,all
ksel,all

ksel,s,kp,,7
nslk,s
*get,nkp7,node,0,num,max
nsel,all
ksel,all


ksel,s,kp,,8
nslk,s
*get,nkp8,node,0,num,max
nsel,all
ksel,all
FINISH

!*************************************************************
!********************** SOLUTION ****************************
!*************************************************************

/SOL


ANTYPE,0                    ! Specifies the analysis type and restart status and
        "0" means that it Performs a static analysis. Valid for all degrees of
        freedom

NLGEOM,1                    ! Includes large-deflection effects in a static or full
        transient analysis

!AUTOTS, ON
!CNVTOL,U,,0.000001,,0
!CNVTOL,F,,0.0001,,0            ! Sets convergence values for nonlinear
        analyses

!************************************

DK,2, ,0, , , ,UX,UY,UZ,ROTX,ROTZ,  ! Boundary conditions on keypoint 2
DK,3, ,0, , , ,UX,UY,UZ,ROTX,ROTZ,  ! Boundary conditions on keypoint 2
```

Appendix A (Continued)

```
DK,8, ,0, , , ,UX,UY,UZ,ROTZ,
LOCAL,11,CART,0,0,0,-44,0,0,
CSYS,11
DK,8,ROTY,0
CSYS,0

!***********************************
*DIM,my1,TABLE,10000

lsnum =0

*DO,step,1,215,15
        theta=-1*step
        DK,2,ROTY,theta*PI/180
        lsnum=lsnum+1
        LSWRITE,lsnum
*ENDDO
stop1 = lsnum


DKDELE,2,ROTY

*DO,step,-15100,15900,100                    !Maximum Moment Value -
        2.1065e+004
        mmy1 = step*1
        FK,2,MY,mmy1


      lsnum=lsnum+1
      *set,MY1(lsnum),step*1

        LSWRITE,lsnum
*ENDDO

FKDELE,2,my

*DO,step,-56,-25,1
        theta=1*step
        DK,2,ROTY,theta*PI/180
        lsnum=lsnum+1
        LSWRITE,lsnum
*ENDDO
```

Appendix A (Continued)

```
DKDELE,2,ROTY

*DO,step,12925,16975,25                    !Maximum Moment Value -
        2.1065e+004
        mmy1 = step*1
        FK,2,MY,mmy1

      lsnum=lsnum+1
      *set,MY1(lsnum),step*1

        LSWRITE,lsnum
*ENDDO

FKDELE,2,my

*DO,step,-39,-180,-1
        theta=1*step
        DK,2,ROTY,theta*PI/180
        lsnum=lsnum+1
        LSWRITE,lsnum
*ENDDO

!*DO,step,-24,-30,-1
        !theta=1*step
        !DK,2,ROTY,theta*PI/180
        !lsnum=lsnum+1
        !LSWRITE,lsnum
!*ENDDO


!*DO,step,-30,-180,-1
        !theta=1*step
        !DK,2,ROTY,theta*PI/180
        !lsnum=lsnum+1
        !LSWRITE,lsnum
!*ENDDO

*Do,nn,1,lsnum

LSSOLVE,nn
/output,progress,txt,,append
*VWRITE,nn              ! Writes data to a file in a formatted sequence
```

Appendix A (Continued)

```
%16.8G

/output
*enddo


/STATUS,SOLU
FINISH
!*****************************
!******* GET RESULTS *********
!*****************************
loadSteps=lsnum
/POST1
*DIM,rotY2,TABLE,loadSteps
*DIM,disX3,TABLE,loadSteps
*DIM,disY3,TABLE,loadSteps
*DIM,disZ3,TABLE,loadSteps
*DIM,disX5,TABLE,loadSteps
*DIM,disY5,TABLE,loadSteps
*DIM,disZ5,TABLE,loadSteps

!*DIM,fx1,TABLE,loadSteps
!*DIM,fy1,TABLE,loadSteps
!*DIM,fz1,TABLE,loadSteps
!*DIM,mx1,TABLE,loadSteps
!*DIM,mz1,TABLE,loadSteps
*DIM,momy2,TABLE,loadSteps

!*DIM,fx2,TABLE,loadSteps

!*DIM,fy2,TABLE,loadSteps
!*DIM,fz2,TABLE,loadSteps
!*DIM,mx2,TABLE,loadSteps
!*DIM,my2,TABLE,loadSteps
!*DIM,mz2,TABLE,loadSteps

!*DIM,fx3,TABLE,loadSteps
!*DIM,fy3,TABLE,loadSteps
!*DIM,fz3,TABLE,loadSteps
!*DIM,mx3,TABLE,loadSteps
!*DIM,my3,TABLE,loadSteps
!*DIM,mz3,TABLE,loadSteps
```

Appendix A (Continued)

```
!*DIM,fx5,TABLE,loadSteps
!*DIM,fy5,TABLE,loadSteps
!*DIM,fz5,TABLE,loadSteps
!*DIM,mx5,TABLE,loadSteps
!*DIM,my5,TABLE,loadSteps
!*DIM,mz5,TABLE,loadSteps

*Do,nn,1,lsnum
set,nn
*GET,roty,Node,nkp2,ROT,Y
*SET,rotY2(nn),roty
*GET,my2,Node,nkp2,RF,MY
*SET,MOMY2(nn),my2

*ENDDO

/output,output_arc%arclength%_asp%aspect%,txt,,

*MSG,INFO,'t','w','R','E','arclength'          ! Writes an output message via the
        ANSYS message subroutine
%-8C %-8C %-8C %-8C %-8C

*VWRITE,h2,b2,R,E2,arclength                   ! Writes data to a file in a formatted
        sequence
%16.8G %-16.8G %-16.8G %-16.8G %-16.8G

*MSG,INFO,'roty2','my1','my2'
%-8C %-8C




*VWRITE,rotY2(1),MY1(1),MOMY2(1)
%16.8G %-16.8G %-16.8G
/output


FINISH

!*ENDDO
!*ENDDO
```

Appendix A (Continued)

Batch File 3

```
!***********************************
/CONFIG,NRES,1000000
!/CWD,'C:\Documents and Settings\aleon2\Desktop\Work'

!***********************************



!***************************************
!******* Set Up Model Variables *********
!***************************************



!*DO,asp, .1,.7,.3
!asp =.1
!aspect    = 10*asp
!*DO,arclength,1,120,1
!arclength=10

/title,3D Beam Non-linear Deflection
/PREP7
!LCLEAR, ALL
!LDELE, ALL
!KDELE, ALL

R=313.38  ! length in micrometers
PI=acos(-1.)
h1=2
b1=20


b2=5
h2=2

b3=27.6
h3=2

!*********** Area properties **************
```

Appendix A (Continued)

```
A1 = h1*b1

Iy1= 1/12*b1*h1*h1*h1
Iz1= 1/12*h1*b1*b1*b1

E1= 169E3  ! Young's modulus in MPa, Force will be micro Newtons

!************************************

A2=  h2*b2

Iz2= 1/12*h2*b2*b2*b2
Iy2= 1/12*b2*h2*h2*h2

E2= 169e3

!************************************

A3=  h3*b3

Iz3= 1/12*h3*b3*b3*b3
Iy3= 1/12*b3*h3*h3*h3

E3= 169e3


!********** Declare an element type: Beam 4 (3D Elastic) *********

ET,1,BEAM4
KEYOPT,1,2,1
KEYOPT,1,6,1


!********** Set Real Constants and Material Properties *********


R,1,A1,Iy1,Iz1,h1,b1, ,          !******Check on the assumptions being made ******

R,2,A2,Iy2,Iz2,h2,b2, ,

R,3,A3,Iy3,Iz3,h3,b3, ,
MPTEMP,1,0
```

Appendix A (Continued)

```
MPDATA,EX,1,,E1
MPDATA,PRXY,1,,0.35              ! Material properties for material 1 and 2

MPTEMP,1,0
MPDATA,EX,2,,E2
MPDATA,PRXY,2,,0.35

MPTEMP,1,0
MPDATA,EX,3,,E3
MPDATA,PRXY,3,,0.35

!***********************************


!********** Create Keypoints 1 throug 7: K(Point #, X-Coord, Y-Coord, Z-Coord)
         *********

K,1,0,0,0,
K,2,0,-235,0,
K,3,0,-60,0,
K,4,0,60,0,
K,5,R*cos(PI/180*72),R*SIN(PI/180*72),0,
K,6,R*cos(PI/180*33),R*sin(PI/180*33),0,
K,7,R*cos(PI/180*29),R*sin(PI/180*29),0,
K,8,R*cos(PI/180*44),-R*sin(PI/180*44),0,


!********* Create Beam using Lines and Arcs and divide into segments *********

LSTR,      2,      3
LSTR,      4,      5
LSTR,      3,      4              ! Draws lines connecting keypoints 1 through 7
LSTR,      6,      7
LARC,5,6,1,R,                     ! Defines a circular arc


LARC,7,8,1,R,
LESIZE,ALL,,,15                   ! Specifies the divisions and spacing ratio on
         unmeshed lines, *****Try making 32 smaller
```

Appendix A (Continued)

```
!********** MESH **********

real,3                  ! Use real constant set 3
type,1                  ! Use element type 1
mat,3                   ! use material property set 3
LMESH,1,2               ! mesh lines 1-2

real,2                  ! Use real constant set 2
type,1                  ! Use element type 1
mat,2                   ! use material property set 2
LMESH,3,4               ! mesh line 3-4

real,1                  ! Use real constant set 1
type,1                  ! Use element type 1
mat,1                   ! use material property set 1
LMESH,5,6               ! mesh line 5-6


!******* Get Node Numbers at chosen keypoints *******


ksel,s,kp,,2
nslk,s
*get,nkp2,node,0,num,max          ! Retrieves a value and stores it as a scalar
        parameter or part of an array parameter**********
nsel,all
ksel,all

ksel,s,kp,,3
nslk,s
*get,nkp3,node,0,num,max
nsel,all
ksel,all

ksel,s,kp,,4
nslk,s
*get,nkp4,node,0,num,max
nsel,all


ksel,all
ksel,s,kp,,5
```

Appendix A (Continued)

```
nslk,s
*get,nkp5,node,0,num,max
nsel,all
ksel,all

ksel,s,kp,,6
nslk,s
*get,nkp6,node,0,num,max
nsel,all
ksel,all

ksel,s,kp,,7
nslk,s
*get,nkp7,node,0,num,max
nsel,all
ksel,all


ksel,s,kp,,8
nslk,s
*get,nkp8,node,0,num,max
nsel,all
ksel,all
FINISH

!*************************************************************
!********************** SOLUTION ****************************
!*************************************************************

/SOL
ANTYPE,0                    ! Specifies the analysis type and restart status and
        "0" means that it Performs a static analysis. Valid for all degrees of
        freedom

NLGEOM,1                    ! Includes large-deflection effects in a static or full
        transient analysis

!AUTOTS, ON
!CNVTOL,U,,0.000001,,0
```

Appendix A (Continued)

```
!CNVTOL,F,,0.0001,,0              ! Sets convergence values for nonlinear
        analyses

!***********************************

DK,2, ,0, , , ,UX,UY,UZ,ROTX,ROTZ,  ! Boundary conditions on keypoint 2
DK,3, ,0, , , ,UX,UY,UZ,ROTX,ROTZ,  ! Boundary conditions on keypoint 2

DK,8, ,0, , , ,UX,UY,UZ,ROTZ,
LOCAL,11,CART,0,0,0,-44,0,0,
CSYS,11
DK,8,ROTY,0
CSYS,0

!***********************************
*DIM,my1,TABLE,10000

lsnum =0

*DO,step,1,149,1
        theta=-1*step
        DK,2,ROTY,theta*PI/180
        lsnum=lsnum+1
        LSWRITE,lsnum
*ENDDO
stop1 = lsnum



DKDELE,2,ROTY

*DO,step,-9400,30200,200
        mmy1 = step*1
        FK,2,MY,mmy1

      lsnum=lsnum+1
      *set,MY1(lsnum),step*1

        LSWRITE,lsnum
*ENDDO
*DO,step,30200,30500,100
```

Appendix A (Continued)

```
        mmy1 = step*1
        FK,2,MY,mmy1

      lsnum=lsnum+1
      *set,MY1(lsnum),step*1

        LSWRITE,lsnum
*ENDDO



FKDELE,2,my

*DO,step,-58,-24,1
        theta=1*step
        DK,2,ROTY,theta*PI/180
        lsnum=lsnum+1
        LSWRITE,lsnum
*ENDDO

DKDELE,2,ROTY

*DO,step,31350,33075,25                    !Maximum Moment Value -
        2.1065e+004
        mmy1 = step*1
        FK,2,MY,mmy1

      lsnum=lsnum+1
      *set,MY1(lsnum),step*1

        LSWRITE,lsnum
*ENDDO

FKDELE,2,my

*DO,step,-28,-180,-1
        theta=1*step
        DK,2,ROTY,theta*PI/180
        lsnum=lsnum+1
        LSWRITE,lsnum
*ENDDO
```

Appendix A (Continued)

```
!*DO,step,-24,-30,-1
        !theta=1*step
        !DK,2,ROTY,theta*PI/180
        !lsnum=lsnum+1
        !LSWRITE,lsnum
!*ENDDO

!*DO,step,-30,-180,-1
        !theta=1*step
        !DK,2,ROTY,theta*PI/180
        !lsnum=lsnum+1
        !LSWRITE,lsnum
!*ENDDO

*Do,nn,1,lsnum

LSSOLVE,nn

/output,progress,txt,,append
*VWRITE,nn              ! Writes data to a file in a formatted sequence
%16.8G

/output
*enddo
/STATUS,SOLU
FINISH

!*****************************
!******* GET RESULTS *********
!*****************************
loadSteps=lsnum
/POST1
*DIM,rotY2,TABLE,loadSteps
*DIM,disX3,TABLE,loadSteps
*DIM,disY3,TABLE,loadSteps
*DIM,disZ3,TABLE,loadSteps
*DIM,disX5,TABLE,loadSteps
*DIM,disY5,TABLE,loadSteps
*DIM,disZ5,TABLE,loadSteps

!*DIM,fx1,TABLE,loadSteps
```

Appendix A (Continued)

```
!*DIM,fy1,TABLE,loadSteps
!*DIM,fz1,TABLE,loadSteps
!*DIM,mx1,TABLE,loadSteps
!*DIM,mz1,TABLE,loadSteps
*DIM,momy2,TABLE,loadSteps

!*DIM,fx2,TABLE,loadSteps
!*DIM,fy2,TABLE,loadSteps
!*DIM,fz2,TABLE,loadSteps
!*DIM,mx2,TABLE,loadSteps
!*DIM,my2,TABLE,loadSteps
!*DIM,mz2,TABLE,loadSteps

!*DIM,fx3,TABLE,loadSteps
!*DIM,fy3,TABLE,loadSteps
!*DIM,fz3,TABLE,loadSteps
!*DIM,mx3,TABLE,loadSteps
!*DIM,my3,TABLE,loadSteps
!*DIM,mz3,TABLE,loadSteps

!*DIM,fx5,TABLE,loadSteps
!*DIM,fy5,TABLE,loadSteps
!*DIM,fz5,TABLE,loadSteps
!*DIM,mx5,TABLE,loadSteps
!*DIM,my5,TABLE,loadSteps
!*DIM,mz5,TABLE,loadSteps

*Do,nn,1,lsnum
set,nn
*GET,roty,Node,nkp2,ROT,Y
*SET,rotY2(nn),roty
*GET,my2,Node,nkp2,RF,MY
*SET,MOMY2(nn),my2

*ENDDO

/output,output_arc%arclength%_asp%aspect%,txt,,

*MSG,INFO,'t','w','R','E','arclength'          ! Writes an output message via the
        ANSYS message subroutine
%-8C %-8C %-8C %-8C %-8C
```

Appendix A (Continued)

```
*VWRITE,h2,b2,R,E2,arclength                    ! Writes data to a file in a formatted
        sequence
%16.8G %-16.8G %-16.8G %-16.8G %-16.8G

*MSG,INFO,'roty2','my1','my2'
%-8C %-8C


*VWRITE,rotY2(1),MY1(1),MOMY2(1)
%16.8G %-16.8G %-16.8G
/output


FINISH

!*ENDDO
!*ENDDO
```

Appendix B: Output ANSYS Text Files

The following files are text files outputted by ANSYS when running the previous batch files

Output to batch 1:

t w R E arclengt

2.0000000 5.0000000 313.38000

roty2 my1

-1.74532925E-02 0.0000000 -223.33658

-3.49065850E-02 0.0000000 -446.66746

-5.23598776E-02 0.0000000 -669.98624

-6.98131701E-02 0.0000000 -893.28688

-8.72664626E-02 0.0000000 -1116.5633

-0.10471976 0.0000000 -1339.8094

-0.12217305 0.0000000 -1563.0190

-0.13962634 0.0000000 -1786.1859

-0.15707963 0.0000000 -2009.3040

-0.17453293 0.0000000 -2232.3668

-0.19198622 0.0000000 -2455.3680

-0.20943951 0.0000000 -2678.3012

-0.22689280 0.0000000 -2901.1599

-0.26179939 0.0000000 -3346.6269

Appendix B (continued)

-0.27925268	0.0000000	-3569.2216
-0.29670597	0.0000000	-3791.7147
-0.31415927	0.0000000	-4014.0989
-0.33161256	0.0000000	-4236.3671
-0.34906585	0.0000000	-4458.5119
-0.36651914	0.0000000	-4680.5257
-0.38397244	0.0000000	-4902.4008
-0.40142573	0.0000000	-5124.1293
-0.41887902	0.0000000	-5345.7032
-0.43633231	0.0000000	-5567.1141
-0.45378561	0.0000000	-5788.3536
-0.47123890	0.0000000	-6009.4127
-0.48869219	0.0000000	-6230.2827
-0.50614548	0.0000000	-6450.9542
-0.52359878	0.0000000	-6671.4176
-0.54105207	0.0000000	-6891.6632
-0.55850536	0.0000000	-7111.6808
-0.57595865	0.0000000	-7331.4599
-0.59341195	0.0000000	-7550.9898
-0.61086524	0.0000000	-7770.2592
-0.62831853	0.0000000	-7989.2566

Appendix B (continued)

-0.64577182	0.0000000	-8207.9700
-0.66322512	0.0000000	-8426.3871
-0.68067841	0.0000000	-8644.4949
-0.69813170	0.0000000	-8862.2802
-0.71558499	0.0000000	-9079.7292
-0.73303829	0.0000000	-9296.8274
-0.75049158	0.0000000	-9513.5600
-0.76794487	0.0000000	-9729.9115
-0.78539816	0.0000000	-9945.8657
-0.80285146	0.0000000	-10161.406
-0.82030475	0.0000000	-10376.515
-0.83775804	0.0000000	-10591.174
-0.85521133	0.0000000	-10805.364
-0.87266463	0.0000000	-11019.066
-0.89011792	0.0000000	-11232.258
-0.90757121	0.0000000	-11444.921
-0.92502450	0.0000000	-11657.029
-0.94247780	0.0000000	-11868.562
-0.95993109	0.0000000	-12079.493
-0.97738438	0.0000000	-12289.797
-0.99483767	0.0000000	-12499.447

Appendix B (continued)

-1.0122910	0.0000000	-12708.415
-1.0297443	0.0000000	-12916.672
-1.0471975	0.0000000	-13124.186
-1.0646508	0.0000000	-13330.926
-1.0821041	0.0000000	-13536.856
-1.0995574	0.0000000	-13741.943
-1.1170107	0.0000000	-13946.148
-1.1344640	0.0000000	-14149.431
-1.1519173	0.0000000	-14351.753
-1.1693706	0.0000000	-14553.069
-1.1868239	0.0000000	-14753.333
-1.2042772	0.0000000	-14952.499
-1.2217305	0.0000000	-15150.516
-1.2391838	0.0000000	-15347.329
-1.2566371	0.0000000	-15542.885
-1.2740903	0.0000000	-15737.123
-1.2915436	0.0000000	-15929.982
-1.3089969	0.0000000	-16121.396
-1.3264502	0.0000000	-16311.297
-1.3439035	0.0000000	-16499.612
-1.3613568	0.0000000	-16686.263

Appendix B (continued)

-1.3788101	0.0000000	-16871.171
-1.3962634	0.0000000	-17054.248
-1.4137167	0.0000000	-17235.406
-1.4311700	0.0000000	-17414.548
-1.4486233	0.0000000	-17591.573
-1.4660766	0.0000000	-17766.375
-1.4835299	0.0000000	-17938.840
-1.5009832	0.0000000	-18108.849
-1.5184364	0.0000000	-18276.275
-1.5358897	0.0000000	-18440.984
-1.5533430	0.0000000	-18602.834
-1.5707963	0.0000000	-18761.676
-1.5882496	0.0000000	-18917.349
-1.6057029	0.0000000	-19069.685
-1.6231562	0.0000000	-19218.505
-1.6406095	0.0000000	-19363.619
-1.6580628	0.0000000	-19504.827
-1.6755161	0.0000000	-19641.916
-1.6929694	0.0000000	-19774.659
-1.7104227	0.0000000	-19902.817
-1.7278760	0.0000000	-20026.136

Appendix B (continued)

-1.7453292	0.0000000	-20144.347
-1.7627825	0.0000000	-20257.165
-1.7802358	0.0000000	-20364.287
-1.7976891	0.0000000	-20465.393
-1.8151424	0.0000000	-20560.143
-1.8325957	0.0000000	-20648.179
-1.8500490	0.0000000	-20729.119
-1.8675023	0.0000000	-20802.562
-1.8849556	0.0000000	-20868.081
-1.9024089	0.0000000	-20925.226
-1.9198622	0.0000000	-20973.523
-1.9373155	0.0000000	-21012.470
-1.9547688	0.0000000	-21041.538
-1.9722220	0.0000000	-21060.171
-1.9896753	0.0000000	-21067.780
-2.0071286	0.0000000	-21063.752
-2.0245819	0.0000000	-21047.437
-2.0420352	0.0000000	-21013.354
-2.0594885	0.0000000	-20969.903
-2.0769418	0.0000000	-20911.976
-2.0943951	0.0000000	-20838.789

Appendix B (continued)

-2.1116863	-20750.000	-20838.789
-2.1491990	-20500.000	-20838.789
-2.1779545	-20250.000	-20838.789
-2.2018684	-20000.000	-20838.789
-2.2225688	-19750.000	-20838.789
-2.2409992	-19500.000	-20838.789
-2.2576922	-19250.000	-20838.789
-2.2730046	-19000.000	-20838.789
-2.2871865	-18750.000	-20838.789
-2.3004208	-18500.000	-20838.789
-2.3128456	-18250.000	-20838.789
-2.3245683	-18000.000	-20838.789
-2.3356739	-17750.000	-20838.789
-2.3462310	-17500.000	-20838.789
-2.3562959	-17250.000	-20838.789
-2.3659153	-17000.000	-20838.789
-2.3751281	-16750.000	-20838.789
-2.3839673	-16500.000	-20838.789
-2.3926752	-16250.000	-20838.789
-2.4008369	-16000.000	-20838.789
-2.4086915	-15750.000	-20838.789

Appendix B (continued)

-2.4162653	-15500.000	-20838.789
-2.4235734	-15250.000	-20838.789
-2.4306291	-15000.000	-20838.789
-2.4374441	-14750.000	-20838.789
-2.4440285	-14500.000	-20838.789
-2.4503913	-14250.000	-20838.789
-2.4565402	-14000.000	-20838.789
-2.4624818	-13750.000	-20838.789
-2.4682222	-13500.000	-20838.789
-2.4737662	-13250.000	-20838.789
-2.4791184	-13000.000	-20838.789
-2.4842823	-12750.000	-20838.789
-2.4892613	-12500.000	-20838.789
-2.4940578	-12250.000	-20838.789
-2.4986743	-12000.000	-20838.789
-2.5031124	-11750.000	-20838.789
-2.5073737	-11500.000	-20838.789
-2.5114593	-11250.000	-20838.789
-2.5153699	-11000.000	-20838.789
-2.5191064	-10750.000	-20838.789
-2.5226689	-10500.000	-20838.789

Appendix B (continued)

-2.5260578	-10250.000	-20838.789
-2.5292730	-10000.000	-20838.789
-2.5323146	-9750.0000	-20838.789
-2.5351823	-9500.0000	-20838.789
-2.5378759	-9250.0000	-20838.789
-2.5403950	-9000.0000	-20838.789
-2.5427394	-8750.0000	-20838.789
-2.5449086	-8500.0000	-20838.789
-2.5469023	-8250.0000	-20838.789
-2.5487202	-8000.0000	-20838.789
-2.5503619	-7750.0000	-20838.789
-2.5518274	-7500.0000	-20838.789
-2.5531163	-7250.0000	-20838.789
-2.5542287	-7000.0000	-20838.789
-2.5551646	-6750.0000	-20838.789
-2.5559241	-6500.0000	-20838.789
-2.5565074	-6250.0000	-20838.789
-2.5569150	-6000.0000	-20838.789
-2.5571473	-5750.0000	-20838.789
-2.5572050	-5500.0000	-20838.789
-2.5570888	-5250.0000	-20838.789

Appendix B (continued)

-2.5567996	-5000.0000	-20838.789
-2.5563384	-4750.0000	-20838.789
-2.5557065	-4500.0000	-20838.789
-2.5549050	-4250.0000	-20838.789
-2.5539353	-4000.0000	-20838.789
-2.5527990	-3750.0000	-20838.789
-2.5514978	-3500.0000	-20838.789
-2.5500332	-3250.0000	-20838.789
-2.5484073	-3000.0000	-20838.789
-2.5466218	-2750.0000	-20838.789
-2.5446788	-2500.0000	-20838.789
-2.5425803	-2250.0000	-20838.789
-2.5403286	-2000.0000	-20838.789
-2.5379256	-1750.0000	-20838.789
-2.5353738	-1500.0000	-20838.789
-2.5326754	-1250.0000	-20838.789
-2.5298326	-1000.0000	-20838.789
-2.5268478	-750.00000	-20838.789
-2.5237233	-500.00000	-20838.789
-2.5204615	-250.00000	-20838.789
-2.5170647	0.0000000	-20838.789

Appendix B (continued)

-2.5135352	250.00000	-20838.789
-2.5098753	500.00000	-20838.789
-2.5060873	750.00000	-20838.789
-2.5021736	1000.0000	-20838.789
-2.4981362	1250.0000	-20838.789
-2.4939775	1500.0000	-20838.789
-2.4896995	1750.0000	-20838.789
-2.4853045	2000.0000	-20838.789
-2.4807944	2250.0000	-20838.789
-2.4761714	2500.0000	-20838.789
-2.4714372	2750.0000	-20838.789
-2.4665939	3000.0000	-20838.789
-2.4616434	3250.0000	-20838.789
-2.4565874	3500.0000	-20838.789
-2.4514276	3750.0000	-20838.789
-2.4461657	4000.0000	-20838.789
-2.4408034	4250.0000	-20838.789
-2.4353422	4500.0000	-20838.789
-2.4297836	4750.0000	-20838.789
-2.4241290	5000.0000	-20838.789
-2.4183798	5250.0000	-20838.789

Appendix B (continued)

-2.4125372	5500.0000	-20838.789
-2.4066026	5750.0000	-20838.789
-2.4005771	6000.0000	-20838.789
-2.3944618	6250.0000	-20838.789
-2.3882578	6500.0000	-20838.789
-2.3819660	6750.0000	-20838.789
-2.3755875	7000.0000	-20838.789
-2.3691230	7250.0000	-20838.789
-2.3625734	7500.0000	-20838.789
-2.3559395	7750.0000	-20838.789
-2.3492219	8000.0000	-20838.789
-2.3424212	8250.0000	-20838.789
-2.3355382	8500.0000	-20838.789
-2.3285733	8750.0000	-20838.789
-2.3215270	9000.0000	-20838.789
-2.3143997	9250.0000	-20838.789
-2.3071917	9500.0000	-20838.789
-2.2999036	9750.0000	-20838.789
-2.2925354	10000.000	-20838.789
-2.2850874	10250.000	-20838.789
-2.2775598	10500.000	-20838.789

Appendix B (continued)

-2.2699527	10750.000	-20838.789
-2.2622662	11000.000	-20838.789
-2.2545004	11250.000	-20838.789
-2.2466552	11500.000	-20838.789
-2.2387305	11750.000	-20838.789
-2.2307263	12000.000	-20838.789
-2.2226425	12250.000	-20838.789
-2.2144788	12500.000	-20838.789
-2.2062350	12750.000	-20838.789
-2.1979108	13000.000	-20838.789
-2.1895059	13250.000	-20838.789
-2.1810201	13500.000	-20838.789
-2.1724528	13750.000	-20838.789
-2.1638037	14000.000	-20838.789
-2.1550723	14250.000	-20838.789
-2.1462580	14500.000	-20838.789
-2.1373605	14750.000	-20838.789
-2.1283789	15000.000	-20838.789
-2.1193129	15250.000	-20838.789
-2.1101616	15500.000	-20838.789
-2.1009245	15750.000	-20838.789

Appendix B (continued)

-2.0916007	16000.000	-20838.789
-2.0821896	16250.000	-20838.789
-2.0726903	16500.000	-20838.789
-2.0631020	16750.000	-20838.789
-2.0534238	17000.000	-20838.789
-2.0436550	17250.000	-20838.789
-2.0337944	17500.000	-20838.789
-2.0238412	17750.000	-20838.789
-2.0137943	18000.000	-20838.789
-2.0036528	18250.000	-20838.789
-1.9934155	18500.000	-20838.789
-1.9830814	18750.000	-20838.789
-1.9726493	19000.000	-20838.789
-1.9621180	19250.000	-20838.789
-1.9514863	19500.000	-20838.789
-1.9407530	19750.000	-20838.789
-1.9299167	20000.000	-20838.789
-1.9189761	20250.000	-20838.789
-1.9079298	20500.000	-20838.789
-1.8967765	20750.000	-20838.789
-1.8855145	21000.000	-20838.789

Appendix B (continued)

-1.8741424	21250.000	-20838.789
-1.8626585	21500.000	-20838.789
-1.8510613	21750.000	-20838.789
-1.8393489	22000.000	-20838.789
-1.8275197	22250.000	-20838.789
-1.8155716	22500.000	-20838.789
-1.8035027	22750.000	-20838.789
-1.7913110	23000.000	-20838.789
-1.7789943	23250.000	-20838.789
-1.7665503	23500.000	-20838.789
-1.7539766	23750.000	-20838.789
-1.7414670	24000.000	-20838.789
-1.7286321	24250.000	-20838.789
-1.7153217	24500.000	-20838.789
-1.7023682	24750.000	-20838.789
-1.6892914	25000.000	-20838.789
-1.6758923	25250.000	-20838.789
-1.6623305	25500.000	-20838.789
-1.6486299	25750.000	-20838.789
-1.6347536	26000.000	-20838.789
-1.6207163	26250.000	-20838.789

Appendix B (continued)

-1.6065086	26500.000	-20838.789
-1.5921240	26750.000	-20838.789
-1.5775557	27000.000	-20838.789
-1.5627838	27250.000	-20838.789
-1.5478262	27500.000	-20838.789
-1.5326576	27750.000	-20838.789
-1.5172685	28000.000	-20838.789
-1.5016464	28250.000	-20838.789
-1.4857772	28500.000	-20838.789
-1.4696448	28750.000	-20838.789
-1.4532304	29000.000	-20838.789
-1.4365121	29250.000	-20838.789
-1.4194642	29500.000	-20838.789
-1.4020562	29750.000	-20838.789
-1.3842513	30000.000	-20838.789
-1.3660050	30250.000	-20838.789
-1.3472626	30500.000	-20838.789
-1.3279554	30750.000	-20838.789
-1.3079957	31000.000	-20838.789
-1.2872692	31250.000	-20838.789
-1.2656218	31500.000	-20838.789

Appendix B (continued)

-1.2428387	31750.000	-20838.789
-1.2186097	32000.000	-20838.789
-1.1924378	32250.000	-20838.789
-1.1634605	32500.000	-20838.789
-1.1300314	32750.000	-20838.789
-1.0876665	33000.000	-20838.789
-0.96938944	33250.000	-20838.789
-0.97738438	0.0000000	33239.297
-0.95993109	0.0000000	33216.962
-0.94247780	0.0000000	33183.262
-0.92502450	0.0000000	33137.183
-0.90757121	0.0000000	33080.835
-0.89011792	0.0000000	33016.772
-0.87266463	0.0000000	32947.893
-0.85521133	0.0000000	32877.319
-0.83775804	0.0000000	32808.231
-0.82030475	0.0000000	32743.724
-0.80285146	0.0000000	32686.672
-0.78539816	0.0000000	32639.630
-0.76794487	0.0000000	32604.778
-0.75049158	0.0000000	32583.894

Appendix B (continued)

-0.69813170	0.0000000	32617.286
-0.68067841	0.0000000	32662.951
-0.66322512	0.0000000	32726.546
-0.64577182	0.0000000	32808.225
-0.62831853	0.0000000	32908.048
-0.61086524	0.0000000	33026.023
-0.59341195	0.0000000	33162.150
-0.57595865	0.0000000	33316.455
-0.55850536	0.0000000	33489.036
-0.54105207	0.0000000	33680.107
-0.52359878	0.0000000	33890.058
-0.50614548	0.0000000	34119.538
-0.48869219	0.0000000	34369.588
-0.47123890	0.0000000	34641.856
-0.45378561	0.0000000	34939.009
-0.43633231	0.0000000	35265.577
-0.41887902	0.0000000	35630.013
-0.40142573	0.0000000	36049.949
-0.38397244	0.0000000	36595.985
-0.38554372	36500.000	36595.985
-0.38585273	36525.000	36595.985

Appendix B (continued)

-0.38515289	36550.000	36595.985
-0.38449126	36575.000	36595.985
-0.38384641	36600.000	36595.985
-0.38321915	36625.000	36595.985
-0.38260998	36650.000	36595.985
-0.38201942	36675.000	36595.985
-0.38144804	36700.000	36595.985
-0.38089643	36725.000	36595.985
-0.38036523	36750.000	36595.985
-0.37985513	36775.000	36595.985
-0.37936686	36800.000	36595.985
-0.37890120	36825.000	36595.985
-0.37845901	36850.000	36595.985
-0.37804118	36875.000	36595.985
-0.37764871	36900.000	36595.985
-0.37728264	36925.000	36595.985
-0.37694414	36950.000	36595.985
-0.37663445	36975.000	36595.985
-0.37635492	37000.000	36595.985
-0.37610705	37025.000	36595.985
-0.37589246	37050.000	36595.985

Appendix B (continued)

-0.37571295	37075.000	36595.985
-0.37557050	37100.000	36595.985
-0.37546730	37125.000	36595.985
-0.37540582	37150.000	36595.985
-0.37538881	37175.000	36595.985
-0.37541939	37200.000	36595.985
-0.37550113	37225.000	36595.985
-0.37563814	37250.000	36595.985
-0.37583525	37275.000	36595.985
-0.37609820	37300.000	36595.985
-0.37643398	37325.000	36595.985
-0.37685140	37350.000	36595.985
-0.37736199	37375.000	36595.985
-0.37798165	37400.000	36595.985
-0.37873359	37425.000	36595.985
-0.37965267	37450.000	36595.985
-0.38010927	37475.000	36595.985
-0.38116689	37500.000	36595.985
-0.38238823	37525.000	36595.985
-0.38314500	37550.000	36595.985
-0.38489833	37575.000	36595.985

Appendix B (continued)

-0.38681297	37600.000	36595.985
-0.38913579	37625.000	36595.985
-0.39195722	37650.000	36595.985
-0.39550168	37675.000	36595.985
-0.40020412	37700.000	36595.985
-0.40714338	37725.000	36595.985
-0.40666172	0.0000000	37712.666
-0.40840705	0.0000000	37716.816
-0.41015237	0.0000000	37719.958
-0.41189770	0.0000000	37722.498
-0.41364303	0.0000000	37724.462
-0.41538836	0.0000000	37725.891
-0.41713369	0.0000000	37726.819
-0.41887902	0.0000000	37727.276
-0.41887902	0.0000000	37727.081
-0.43633231	0.0000000	37710.977
-0.45378561	0.0000000	37667.193
-0.47123890	0.0000000	37604.736
-0.48869219	0.0000000	37528.474
-0.50614548	0.0000000	37441.458
-0.52359878	0.0000000	37345.734

Appendix B (continued)

-0.52359878	0.0000000	37345.734
-0.54105207	0.0000000	37242.754
-0.55850536	0.0000000	37133.583
-0.57595865	0.0000000	37019.033
-0.59341195	0.0000000	36899.733
-0.61086524	0.0000000	36776.183
-0.62831853	0.0000000	36648.787
-0.64577182	0.0000000	36517.876
-0.66322512	0.0000000	36383.722
-0.68067841	0.0000000	36246.555
-0.69813170	0.0000000	36106.693
-0.71558499	0.0000000	35964.045
-0.73303829	0.0000000	35818.884
-0.75049158	0.0000000	35671.327
-0.76794487	0.0000000	35521.477
-0.78539816	0.0000000	35369.425
-0.80285146	0.0000000	35215.250
-0.82030475	0.0000000	35061.914
-0.83775804	0.0000000	34903.497
-0.85521133	0.0000000	34743.280
-0.87266463	0.0000000	34581.162

Appendix B (continued)

-0.89011792	0.0000000	34417.187
-0.90757121	0.0000000	34251.387
-0.92502450	0.0000000	34083.793
-0.94247780	0.0000000	33914.428
-0.95993109	0.0000000	33743.315
-0.97738438	0.0000000	33570.470
-0.99483767	0.0000000	33395.908
-1.0122910	0.0000000	33219.641
-1.0297443	0.0000000	33041.678
-1.0471975	0.0000000	32862.027
-1.0646508	0.0000000	32680.692
-1.0821041	0.0000000	32497.675
-1.0995574	0.0000000	32312.978
-1.1170107	0.0000000	32126.600
-1.1344640	0.0000000	31938.538
-1.1519173	0.0000000	31748.789
-1.1693706	0.0000000	31557.348
-1.1868239	0.0000000	31364.208
-1.2042772	0.0000000	31169.364
-1.2217305	0.0000000	30972.805
-1.2391838	0.0000000	30774.524

Appendix B (continued)

-1.2566371	0.0000000	30574.511
-1.2740903	0.0000000	30372.755
-1.2915436	0.0000000	30169.246
-1.3089969	0.0000000	29963.972
-1.3264502	0.0000000	29756.922
-1.3439035	0.0000000	29548.085
-1.3613568	0.0000000	29337.447
-1.3788101	0.0000000	29124.999
-1.3962634	0.0000000	28910.728
-1.4137167	0.0000000	28694.622
-1.4311700	0.0000000	28476.671
-1.4486233	0.0000000	28256.864
-1.4660766	0.0000000	28035.190
-1.4835299	0.0000000	27811.641
-1.5009832	0.0000000	27586.207
-1.5184364	0.0000000	27358.880
-1.5358897	0.0000000	27129.653
-1.5533430	0.0000000	26898.521
-1.5707963	0.0000000	26665.477
-1.5882496	0.0000000	26430.518
-1.6057029	0.0000000	26193.642

Appendix B (continued)

-1.6231562	0.0000000	25954.846
-1.6406095	0.0000000	25714.131
-1.6580628	0.0000000	25471.497
-1.6755161	0.0000000	25226.948
-1.6929694	0.0000000	24980.487
-1.7104227	0.0000000	24732.120
-1.7278760	0.0000000	24481.854
-1.7453292	0.0000000	24229.697
-1.7627825	0.0000000	23975.659
-1.7802358	0.0000000	23719.751
-1.7976891	0.0000000	23461.986
-1.8151424	0.0000000	23202.379
-1.8325957	0.0000000	22940.945
-1.8500490	0.0000000	22677.701
-1.8675023	0.0000000	22412.665
-1.8849556	0.0000000	22145.856
-1.9024089	0.0000000	21877.296
-1.9198622	0.0000000	21607.006
-1.9373155	0.0000000	21335.009
-1.9547688	0.0000000	21061.329
-1.9722220	0.0000000	20785.989

Appendix B (continued)

-2.0071286	0.0000000	20230.438
-2.0245819	0.0000000	19950.279
-2.0420352	0.0000000	19668.568
-2.0594885	0.0000000	19385.333
-2.0769418	0.0000000	19100.602
-2.0943951	0.0000000	18814.405
-2.1118484	0.0000000	18526.770
-2.1293017	0.0000000	18237.727
-2.1467550	0.0000000	17947.306
-2.1642083	0.0000000	17655.537
-2.1816616	0.0000000	17362.450
-2.1991149	0.0000000	17068.074
-2.2165681	0.0000000	16772.440
-2.2340214	0.0000000	16475.578
-2.2514747	0.0000000	16177.516
-2.2689280	0.0000000	15878.286
-2.2863813	0.0000000	15577.915
-2.3038346	0.0000000	15276.435
-2.3212879	0.0000000	14973.873
-2.3387412	0.0000000	14670.258
-2.3561945	0.0000000	14365.620

Appendix B (continued)

-2.3911011	0.0000000	13753.382
-2.4085544	0.0000000	13445.840
-2.4260077	0.0000000	13137.384
-2.4434609	0.0000000	12828.041
-2.4609143	0.0000000	12517.840
-2.4783675	0.0000000	12206.805
-2.4958208	0.0000000	11894.963
-2.5132741	0.0000000	11582.339
-2.5307274	0.0000000	11268.959
-2.5481807	0.0000000	10954.847
-2.5656340	0.0000000	10640.029
-2.5830873	0.0000000	10324.528
-2.6005406	0.0000000	10008.369
-2.6179939	0.0000000	9691.5748
-2.6354472	0.0000000	9374.1695
-2.6529005	0.0000000	9056.1761
-2.6703538	0.0000000	8737.6170
-2.6878071	0.0000000	8418.5154
-2.7052603	0.0000000	8098.8932
-2.7227136	0.0000000	7778.7726
-2.7401669	0.0000000	7458.1751

Appendix B (continued)

-2.7576202	0.0000000	7137.1227
-2.7750735	0.0000000	6815.6366
-2.7925268	0.0000000	6493.7379
-2.8099801	0.0000000	6171.4474
-2.8274334	0.0000000	5848.7862
-2.8448867	0.0000000	5525.7746
-2.8623400	0.0000000	5202.4332
-2.8797933	0.0000000	4878.7818
-2.8972466	0.0000000	4554.8410
-2.9146998	0.0000000	4230.6305
-2.9321531	0.0000000	3906.1702
-2.9496064	0.0000000	3581.4796
-2.9670597	0.0000000	3256.5785
-2.9845130	0.0000000	2931.4863
-3.0019663	0.0000000	2606.2224
-3.0194196	0.0000000	2280.8059
-3.0368729	0.0000000	1955.2564
-3.0543262	0.0000000	1629.5929
-3.0717795	0.0000000	1303.8345
-3.0892328	0.0000000	978.00002
-3.1066861	0.0000000	652.10892

Appendix B (continued)

-3.1241394	0.0000000	326.18001
-3.1415927	0.0000000	0.23225880

Appendix C: MatLab M-File

The following file is an M-file that is used in MatLab. It reads the output of the ANSYS Batch files.

M-File:

```
%%%%%%%%%%%%%%%%%%%%%%%%%%%%%%%%%%%%%%%%%%%%%%%%%%%%%%%%%%%%%%%%%%%%%%%
% Ansys data analysis file                                              %
% For an Ansys batch file                                               %
% which produces an output file named knee_output.txt                   %
% Version 1: May 18,2007                                                %
%%%%%%%%%%%%%%%%%%%%%%%%%%%%%%%%%%%%%%%%%%%%%%%%%%%%%%%%%%%%%%%%%%%%%%%

 filename = ['output_arc%arclength%_asp%aspect%.txt'];
 string1 =
['C:\DOCUME~1\JOSEPH~1\DESKTOP\MYMAST~1\ANSYS\A7_Optimized\Run5_7square
s_optimized\'];
fid1 = fopen([string1,filename]);    % opens the file
ABT = fread(fid1);                     % reads the file into variable
ABT
fclose(fid1);                         %closes the data file
GBT = native2unicode(ABT)';           %changes data from machine code to
text
s_iB = findstr('my1', GBT);           % finds end of header
A=str2num(GBT(s_iB+4:end))               % turns the data into a
numerical matrix
roty2 = A(:,1);
my2   = A(:,2);
my3   = A(:,3)
figure(1)
plot(roty2*180/pi,[my2,my3],'*')
```